

## Perspectives on chemistries of aqueous and non-aqueous batteries for renewable electricity storage

Olusola O. James<sup>1,\*</sup>, Helen T. Afolayan<sup>1</sup>, Wahab A. Osunniran<sup>1</sup>, Sunday W. Balogun<sup>2</sup>, Tolutope O. Siyanbola<sup>3</sup>

<sup>1</sup>Chemistry Unit, Faculty of Pure & Applied Sciences, Kwara State University, Malete, Nigeria

<sup>2</sup>Department of Materials Science & Engineering, Faculty of Engineering & Technology, Kwara State University, Malete, Nigeria

<sup>3</sup>Department of Chemistry, Covenant University, Ota, Nigeria

**Abstract:** The role of batteries towards mitigating the challenge of intermittent nature of solar and wind electricity supply cannot be over-emphasised. Batteries are essential complements to solar and wind electricity as we seek to increase the proportion of renewable electricity in the global energy mix. Since batteries are devices for chemical-electrical energy inter-conversion, their usefulness depends on chemistry. This makes it imperative to improve on the chemistries of existing commercial batteries for grid-scale electricity storage applications. In this contribution, we examined the chemistries of lead-acid, zinc-alkaline, lithium ion, aluminium and liquid metal batteries vis-à-vis their utility for grid-scale electricity storage. Simple assembly and rugged cell operation are key advantages of lead-acid batteries despite their low specific capacity. Poor cycle life span and low cell voltage are the main weaknesses of zinc-alkaline batteries. Emerging zinc ion batteries with improve cycle life span can make zinc-based batteries suitable for grid-scale applications. Lithium ion batteries are based on rocking chair chemistry and were an instant success for mobile and portable electronics application. Currently, lithium ion batteries are expanding into the electric vehicle applications and other areas. However, grid-scale application of lithium ion batteries will depend on cost and safety. Aluminium emerged from obscurity of Hall-Héroult electrolysis cell to a promising battery material. Emerging aluminium batteries can combine key strengths of zinc ion and lithium ion batteries to carve a sizeable market share including grid-scale application. Liquid metal batteries are grid-scale storage application focused. This battery type has advantages of simple assembly, low materials cost, and long cycle life span. However, high operating temperature and corrosion problems are its weaknesses.

**Keywords:** Battery; grid-scale storage; lithium; zinc; aluminium

### 1. Introduction

Energy is the currency of activities on our planet. All human socio-economic activities involve energy expenditure. Although the sun is the ultimate source of energy on our planet, there are different forms of energy – mechanical, heat, sound, tide, electrical, etc. Early human civilisations were built mainly through exploitations of natural mechanical energy flows using mills (wind & water) and muscle powers (human & animal) (Olugbenga, 2009). Plants supply human and animal with energy needs; plants capture and store

energy from the sun through photosynthesis. The stored (chemical) energy in form of food, biomass, and fossil fuels are important energy reservoirs. Digestion and metabolism of food ingested by animals (including humans) convert energy stored in food into heat and other forms of energy required to sustain life. Animals may be considered complex biological machines that can perform different energy conversions. Combustion of biomass releases stored chemical energy as heat and light energy. Long ago before humans figured out how to construct mills, the art of exploiting biomass combustion for heating, cooking, metallurgy, ceramics,

\* Corresponding author:  
Email: [olusola.james@kwasu.edu.ng](mailto:olusola.james@kwasu.edu.ng)



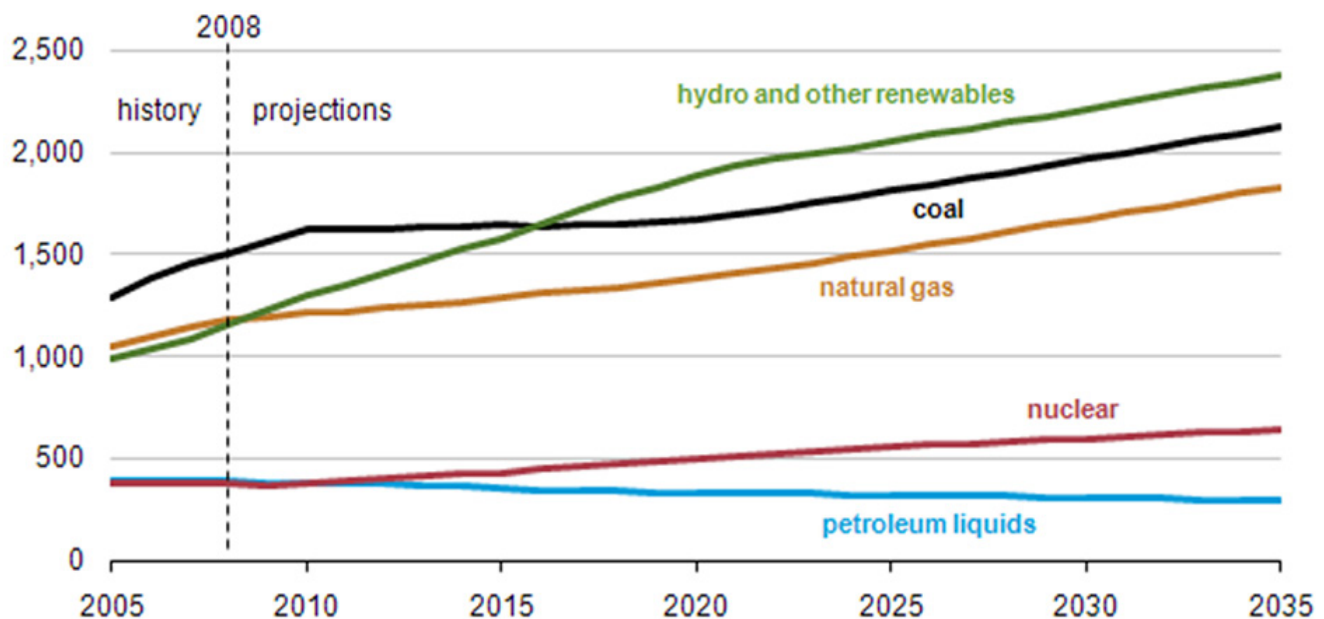
etc., had been perfected. This art was extended to fossil fuels and the invention of heat engines (devices for converting heat energy into mechanical energy) which kick-started the nineteenth century industrial revolution. The industrial revolution in turn propelled evolution from art to science of energy conversions and development of thermodynamics.

The nineteenth century industrial revolution rides on the back of development of engines (steam, diesel & internal combustion). The engine powered industrial revolution dove-tailed into the discovery of electricity and subsequently the invention of the electric motor. An electric motor converts electrical energy into mechanical energy. While engines require fuel(s) to generate mechanical motion, battery is a fuel equivalent for electric motor. Although the invention of the battery by Alexander Volta in 1886 (Yuste, 2008) is a watershed in the investigation of the physics of current electricity, the application of Faraday's law of electromagnetic induction immediately displaced the battery as preferred method of electricity generation. Electromagnetic induction is based on the trio of motion, magnetic field and electric current. The motion required to generate electricity may be obtained from wind, hydro or derived from engines. Global hydroelectricity installations had grown tremendously over the years. Large river bodies are being exploited to execute hydro-electricity projects. From Niagara fall in USA in the 1896 to Aswan dams in 1902, 1976, and more recently Grand Ethiopian

Renaissance Dam under construction, hydroelectricity capacity is still growing. Despite the remarkable growth of installed hydropower, it lagged behind that of coal powered electricity production (Figure 1).

Hydro, nuclear and geothermal energy resources, including wind and solar which are considered renewable sources of electricity generation are increasingly becoming popular in recent times, especially as coal based electricity production (fossil fuels consumption in general) is non-renewable and now poses threats to the climatic order of the planet. This is as increasing carbon emissions from fossil fuels combustion results in greenhouse effect on the planet (Latake et al., 2015). This in turn is causing global warming and climate change. Therefore, a roll-back on fossil fuels consumption is being advocated. As a result, electricity generation from renewable resources are being encouraged (Breeze, 2017; Salameh, 2014). It is projected that before the end of this decade, solar powered electricity capacity will match hydroelectricity capacity and in the next two decades total renewable electricity generation capacity will out-pace that of fossil fuels (Figure 2).

Electricity is a versatile form of energy especially as the demand for electricity is rising rapidly. In fact, a close nexus had been found to exist between wealth and electricity consumption. Wealthy nations consume more electricity and poor countries also strive for increased access to electricity for improved standard of living (Ayres et al., 2013). Solar and wind are the



Source: Global installed electricity generation capacity by energy source (U. S. Energy Information Administration, 2011, September 28)

**Figure 1:** Historic hydropower installed capacity and Global installed electricity generation capacity by energy

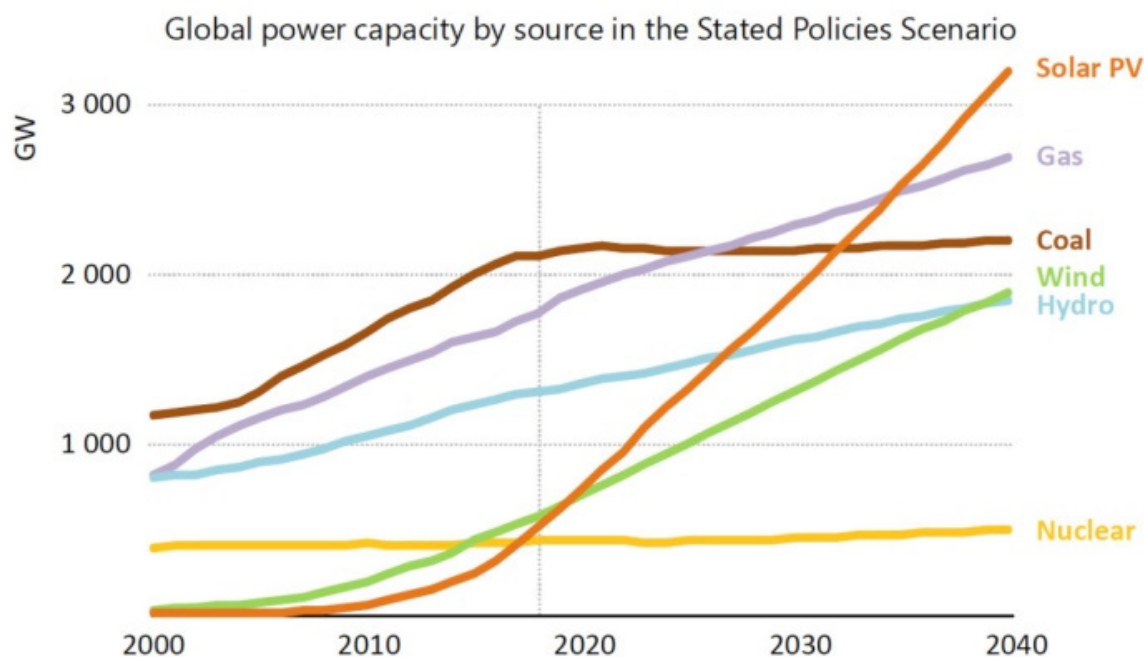


**Figure 2:** International Energy Agency (IEA) world energy outlook - projected global power capacity (Patel 2019)

**Table 1:** Cell reactions for aqueous Zn-Cu battery

| Electrode & cell notation   | Electrode & cell reaction   | Reduction potential |
|---|---|---------------------|
| Zn/Zn <sup>2+</sup>   | $\text{Zn}_{(s)} + 2e \leftrightarrow \text{Zn}^{2+}_{(aq)}$                                      | -0.7618 V           |
| Cu/Cu <sup>2+</sup>   | $\text{Cu}_{(s)} + 2e \leftrightarrow \text{Cu}^{2+}_{(aq)}$                                      | +0.340 V            |
| $\text{Zn}_{(s)}/\text{Zn}^{2+}_{(aq)} / \text{Cu}^{2+}_{(aq)}/\text{Cu}_{(s)}$ | $\text{Zn}_{(s)} + \text{Cu}^{2+}_{(aq)} \leftrightarrow \text{Zn}^{2+}_{(aq)} + \text{Cu}_{(s)}$ | 1.1018 V            |

most abundant and sustainable renewable resources that can be used to satisfy the anticipated growth in electricity demand. However, the full potential of solar and wind electricity cannot be realised without storage (Kirchman, 2008). Solar and wind are intermittent in nature; storage provides the buffer for when the sun is not shining or the wind is not blowing. Using excess solar and wind electricity to perform mechanical (pump-hydro) or chemical (electro-fuels formation) work can serve as large-scale storage. Conversely, pump-hydro suffers from geo-location restrictions, while electro-fuels formation is still in its infancy (Hasanuzzaman et al., 2016). Moreover, overall electricity recovery efficiency of these methods is usually very low due to entropy losses. After its pioneer role as electricity source/storage, battery development had been restricted to small, mobile or portable applications. However, there is a renaissance of interests in battery for large scale electricity (Chen

et al., 2009; Gür, 2018). Therefore, in this report we attempt to examine the chemistries of existing commercial aqueous and non-aqueous batteries for their suitability for grid-scale electricity storage. Also we attempt to dissect the chemistries of new emerging non-aqueous battery technologies vis-à-vis their utility for grid scale electricity storage, but first we give a brief overview on battery.

## 2. Battery: An overview

A battery is an electrical circuit arrangement comprising two electrodes linked together by a metallic and an ionic conductors. An electrode is an electrochemical set-up that allows reversible electron exchange across interfaces (solid-liquid, solid-gas, liquid-gas or liquid-liquid). Usually solid-liquid interface electrode processes are preferred for battery applications. A metal coupon in a solution of its salt is an example of a typical battery electrode. For example, zinc and copper

coupons in contact with respective sulphate solutions. Their notations and electrode processes are shown in Table 1.

A spontaneous redox reaction between the two electrodes will cause electron transfer from one of the electrode (anode) to the other electrode (cathode). The redox reaction is also usually associated with release and uptake of ions by the electrodes and migrations of ions to the electrodes completes the electrical circuit. The consequence of uptake/release of ions has effect on the cell potential according to Nernst equation (equation 1). Keeping the zinc and copper coupons apart is crucial so that the electron transfer of the redox reaction will take place through the connecting metallic conductor and allows for harnessing the electron flow to perform useful work.

$$\text{Nernst equation of the cell } E^o = E_{cell}^o - \frac{RT}{nF} \ln \left( \frac{Zn^{2+}}{Cu^{2+}} \right) \quad (1)$$

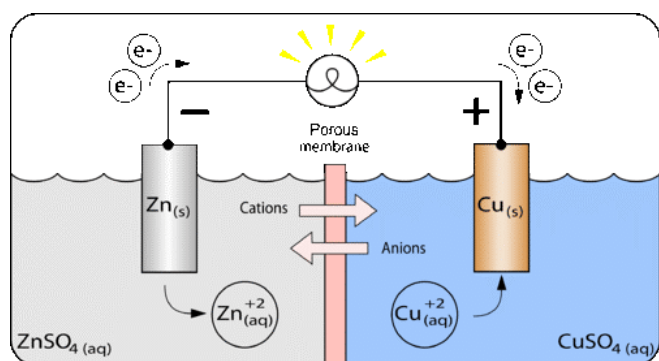


**Figure 3:** Circuit illustration of aqueous Zn-Cu battery (Lumen, 2020)

Salient deductions from Figure 3 which constitute general requirements for achieving battery operation are:

- The electrode terminals/current collectors must be solids (zinc and copper coupons in the case of the cell in Figure 3) and must be electronically conducting.
- There should be large difference between the reduction potentials of the electrodes.
- The electrolyte (sulphate solutions in the case of the cell in Figure 3) should be ionically conducting but electronically insulating.
- In addition to fast reversible electron process, for a rechargeable battery the choice of electrodes and cell assembly should prevent mass loss during discharge and recharge cycle.

Other technical requirements of large-scale energy storage include: high charge storage capacity and specific energy, cycle life, safety and cost. Theoretical charge storage capacity of a cell can be calculated by Faraday's law:

$$\text{Theoretical} = \frac{nF}{3600 \times \text{mass of active material}} \left( \frac{\text{Ah} \cdot \text{s} \cdot \text{mol}^{-1}}{\text{s} \cdot \text{g} \cdot \text{mol}^{-1}} \right) = (\text{mAh g}^{-1}) \quad (2)$$

$$\text{Theoretical specific energy} = Q_{\text{theoretical}} \times E_{\text{cell}}^o = (\text{J} \cdot \text{g}^{-1}) \quad (3)$$

Where  $n$  is the number of electrons,  $F$  is the Faraday constant,  $E_{\text{cell}}^o$  is standard cell potential.

In terms of cost, environmental friendliness, safety, and ease of operation, aqueous battery systems can meet large proportion of the technical requirements of large-scale electricity storage. Thus, in the next section we will first discuss commercial aqueous battery systems.

### 3. Aqueous battery systems

With requirements of cost and safety largely meet, an overriding parameter in aqueous battery systems is energy density. Despite the safety and cost advantages, the aqueous environment imposes two important constraints:

- limitation of potential window of stability region of water, and
- stability of current collector in aqueous media.

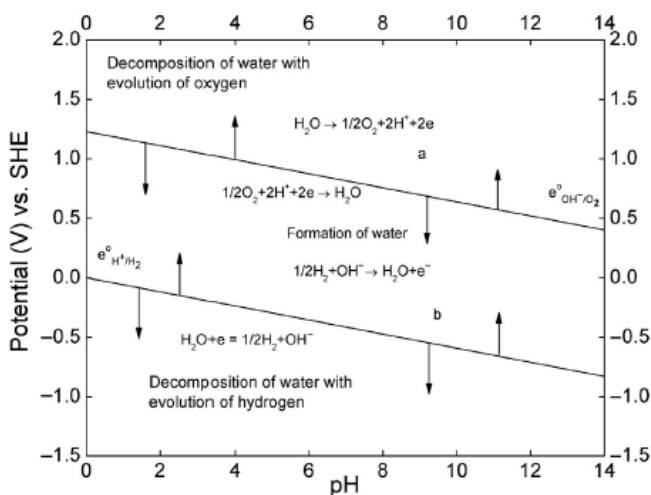
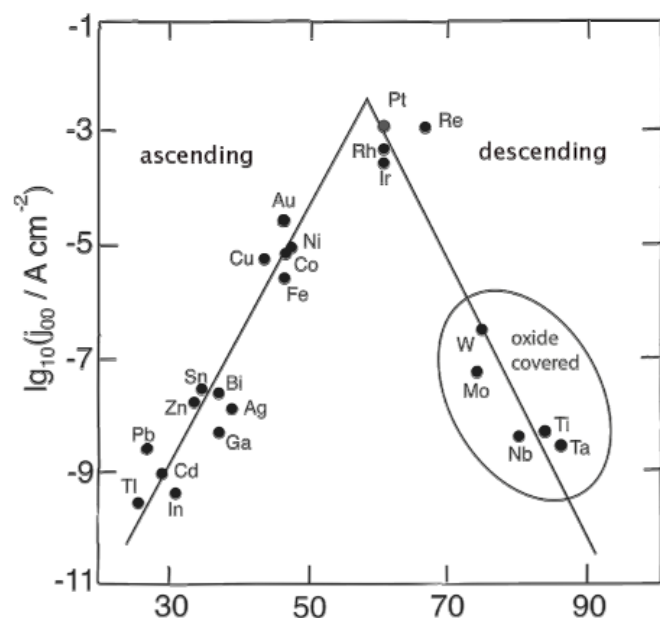


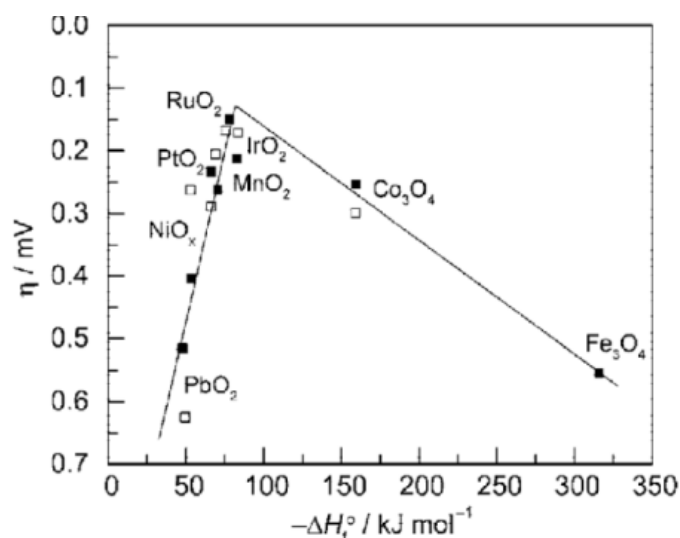
**Figure 4:** Pourbaix diagram for water showing regions for water stability and water electrolysis at STP (Popov, 2015)

The choice of anode and cathode for aqueous battery is restricted to those that have reduction potential within the stability region of water. Figure 4 shows the Pourbaix diagram of water.





a - Volcano plot of  $H_2$  production activity on metal surface vs energy of hydride formation in acid solutions EMH (Quaino et al., 2014)



b - Volcano plot of activity for  $O_2$  production on metal oxide surfaces vs the enthalpy of transition of the oxide in acidic and basic solutions (Trasatti, 1984)

Figure 5: Volcano plots of hydrogen and oxygen evolution reactions

It shows that the potential window of water and thermodynamically battery cell potential in aqueous is limited to 1.23V. The Zn-Cu battery illustrated in Figure 3 operates just with the window with 1.1V cell potential. Thermodynamically, discharge or charging of aqueous battery outside the 1.23V window should be associated with extensive hydrogen and/or oxygen evolution. However, kinetically the potential window can be widened using high over-potential electrodes (hydrogen and oxygen evolution). The volcano plots of hydrogen and oxygen evolution reactions (Figure 5) provide useful guide for selection or rationalising behaviour of electrode metal electrodes for aqueous battery systems. Stability of current collector in aqueous media is another important constraint in the selection of electrode terminals or current collectors for aqueous battery systems. Information on thermodynamic stability of metals in aqueous environment can be obtained from their Pourbaix diagrams. A simple battery system is obtained where product(s) of electrodes reactions are solid and do affect the structural integrity and electronic conductivity of a metal electrode. Where this is not obtainable, a chemically inert but electronically conducting material must be used as terminal or

current collector. The next section explores some of the most successful aqueous batteries.

### 3.1. Lead-acid battery

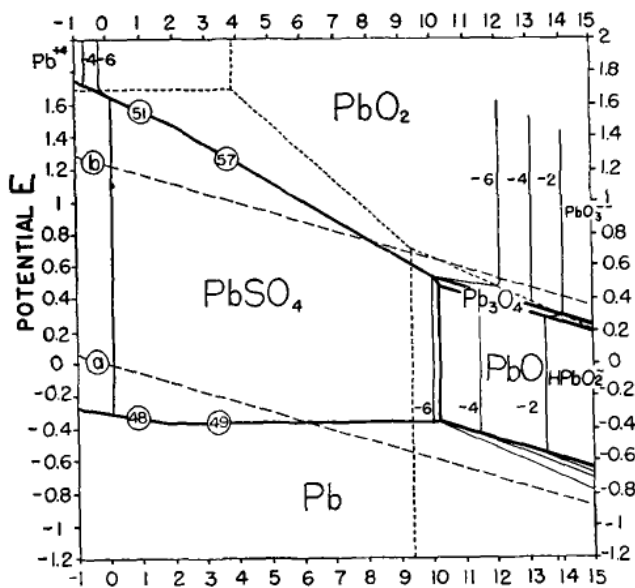
The lead-acid battery is the most commercially successful aqueous battery. Besides its ubiquitous use in automobiles (starting, lighting and ignition), it has also found applications for storage in UPS (uninterrupted power supplies) systems in offices, homes & hospitals, as well as stand-alone power systems. The key factor responsible for the success of lead-acid battery is the unique stability and redox chemistry of lead (Pb) in sulphuric acid solution. Lead is one of few metals that form insoluble sulphate. As shown in Figure 6 an insoluble sulphate passivation develops on the surface of lead when immersed in sulphuric acid solution. Moreover, as depicted in Figure 5, Pb and  $PbO_2$  have high over-potentials for hydrogen and oxygen evolution respectively. The poor kinetics of electrolysis of water over Pb and  $PbO_2$  diminishes the limitation of potential window of water stability. Thus the potential gap of the redox chemistry of lead in sulphuric acid (depicted in Table 2) can be harnessed to obtain cell voltage 2.05V.

**Table 2:** Cell reaction for lead-acid battery

| Electrode | Electrode & cell reaction  | Reduction potential |
|-----------|--|---------------------|
| Anode     | $Pb_{(s)} + HSO_4^-_{(aq)} \longrightarrow PbSO_{4(s)} + H^+_{(aq)} + 2e^-$                  | - 0.36 V            |
| Cathode   | $PbO_{2(s)} + HSO_4^-_{(aq)} + 3H^+_{(aq)} + 2e^- \longrightarrow PbSO_{4(s)} + 2H_2O_{(l)}$ | + 1.69 V            |
| Overall   | $Pb_{(s)} + PbO_{2(s)} + 2HSO_4^-_{(aq)} + 2H^+_{(aq)} \longrightarrow 2PbSO_{4(s)}$         | + 2.05V             |

Nernst equation of the cell 
$$E^o = E^o_{cell} - \frac{RT}{nF} \ln \left( \frac{1}{[H^+]^2 [HSO_4^-]^2} \right) \quad (4)$$

$n = 2, F = 96485 \text{ Asmol}^{-1}, Q_{theoretical} = \frac{2 \times 96485}{3600 \times 642.6} = 83.4 \text{ mAhg}^{-1}$

**Figure 6:** Pourbaix diagram of lead in presence of sulphate ion (Delahay et al., 1951)

Theoretical specific energy =  $83.4 \times 2.05 = 171 \text{ J g}^{-1}$ . In practice, the specific energy will be less than  $171 \text{ J g}^{-1}$  depending on the mass of dead weights (mass of water and package material). The phase and volume change associated with charging and discharge the cell operation result in poor cycling. The challenge of water electrolysis is only minimised but not eliminated. Water electrolysis can also contribute to electrode instability and water loss had to be replenished to maintain the cell electrolyte. In order to improve the cell cycling lead alloys Pb-Ca, and

$PbO_2$ - $Sb_2O_3$  had been employed as anodes and cathodes in some commercial lead-acid batteries (Prengaman, 1991; Venugopalan et al., 1993).  $H_3PO_4$ ,  $Na_2SiO_3$  and recently,  $H_3BO_3$  had also been explored as additive to  $H_2SO_4$  had been found to increase hydrogen and oxygen evolution over-potentials (Pan et al., 2012; Zhongfei et al., 2020). Reduction of water content via use of gel electrolyte reduces dead weights and enhances practical specific energy. Further improvements known as sealed or VRLA (valve-regulated lead-acid) battery system had also been pursued to reduce maintenance cost (Technopark, 2017). Despite the many improvements it is obvious that the charge storage capacity and specific energy of lead-acid battery is low, yet its low cost of materials (lead and sulphuric acid), the simple assembly and rugged cell operation are still very attractive that lead-acid battery commands the top spot in the battery market. The scope of applications is increasing especially stationary applications including grid scale storage.

### 3.2. Zinc-based battery systems

Like lead, due to high over-potential for hydrogen evolution, zinc is another fascinating metal for aqueous battery system. From cost, safety and pollution perspective, zinc is even more attractive than lead. However, the redox chemistry of zinc does not permit simple cell assembly like lead. Zinc does not have exploitable reaction/phase change at oxidising region of its Pourbaix diagram. Hence, another metal/material (as cathode) must be coupled to zinc (as

**Table 3:** Cell reaction for Zn-MnO<sub>2</sub> alkaline battery

| Electrode | Electrode & cell reaction   | Reduction potential |
|-----------|---|---------------------|
| Anode     | $\text{Zn}_{(s)} + 2\text{OH}^-_{(aq)} \rightarrow \text{ZnO}_{(s)} + \text{H}_2\text{O}_{(l)} + 2e^-$              | - 1.28 V            |
| Cathode   | $2\text{MnO}_{2(s)} + \text{H}_2\text{O}_{(l)} + 2e^- \rightarrow \text{Mn}_2\text{O}_{3(s)} + 2\text{OH}^-_{(aq)}$ | +0.15 V             |
| overall   | $\text{Zn}_{(s)} + 2\text{MnO}_{2(s)} \rightleftharpoons \text{ZnO}_{(s)} + \text{Mn}_2\text{O}_{3(s)}$             | +1.43 V             |

Nernst equation of the cell  $E^o = E^o_{cell} \dots(5)$

$$n = 2, F = 96485 \text{ Asmol}^{-1}, Q_{\text{theoretical}} = \frac{2 \times 96485}{3600 \times 152.34} = 351.86 \text{ mAhg}^{-1}$$

Theoretical specific energy =  $351.86 \times 1.43 = 503.16 \text{ J g}^{-1}$ .

anode) in order obtain a battery cell. This requires careful consideration of two Pourbaix diagrams to identify region/condition of mutual stability of the two electrodes. While high hydrogen evolution over-potential of Zn permit minimised hydrogen formation and at significantly high negative reduction potential, a complementary high oxygen evolution over-potential material is desirable as cathode so as to obtain high-energy storage capacity.

### 3.2.1. Zinc-alkaline batteries

Zinc-manganese oxide battery is the second most successful aqueous battery system. As can be seen from Figure 7, zinc and its oxidation product as well as manganese dioxide and its reduction product are stable in alkaline media. The cell reaction is shown in Table 3.

The theoretical charge storage capacity and specific energy of Zn-MnO<sub>2</sub> battery are about quadruple and triple that of lead-acid battery. However, the theoretical storage capacity is not realisable. Unlike in lead-acid battery where both electrodes displayed metallic conductivity, MnO<sub>2</sub> has low electronic conductivity; hence, an inert conducting additive (graphite) is usually added. Moreover, MnO<sub>2</sub> is usually in powdery form and a binder is required for shaping it into a solid. Therefore, cell assembly is not simple and substantial amount of dead weights are integral components of a working Zn-MnO<sub>2</sub> battery. The composite MnO<sub>2</sub> electrodes usually have poor stability in alkali electrolyte. Hence, gel or polymer electrolytes are used in commercial Zn-MnO<sub>2</sub> alkaline batteries most of which are for small portable applications. The solid or semi-solid electrolyte also serves as separator to prevent short-circuiting the battery due to zinc dendrites formation. Yet, there are reports of electrolyte leakages in addition to a major weakness of poor discharge/recharge cycle lifespan.

The incidences of electrolyte leakage and poor discharge/recharge cycle lifespan of Zn-MnO<sub>2</sub> alkaline batteries may be traced to the Pourbaix diagrams of zinc and manganese. As can be deduced from Pourbaix diagram, Zn forms soluble zincate anion at high pH (13-14) electrolyte typically used for Zn-MnO<sub>2</sub> battery. The zincate anion does not migrate back to the cathode during recharging. Similarly, MnO<sub>2</sub> is prone to formation of soluble manganite (VII) anion at high pH during recharging. Organic binder normally used to hold the MnO<sub>2</sub> composite together is prone to attack by the highly oxidising manganite (VII) anion. It is also important to point out that MnO<sub>2</sub> is not far from the peak of the oxygen evolution volcano plot (Figure 5b). At the high pH environment, MnO<sub>2</sub> is a potential oxygen evolution catalyst. Therefore, gas formation is also detrimental to the structural integrity of the composite MnO<sub>2</sub> electrode.

From the above analysis, it is obvious that despite its higher storage capacity the Zn-MnO<sub>2</sub> alkaline battery is not yet a candidate for grid-scale electricity storage. Other materials with similar Pourbaix diagram like MnO<sub>2</sub> (Table 4) had been investigated as cathode for Zn-alkaline batteries but one or more of the challenges highlighted for Zn-MnO<sub>2</sub> is applicable to all of them. To fix the challenges, this will require focus on two key components of the battery, namely: reduce and control the electrolyte pH, enhance electronic conductivity and structural integrity of MnO<sub>2</sub>. Use of alkaline buffer (9-10) as electrolyte will minimise formation of soluble zincate anion. It will also reduce the chance of formation of soluble manganite (VII) anion. Doping MnO<sub>2</sub> with aleoalent cations and reduced graphene oxide may enhance electronic conductivity and structural integrity of MnO<sub>2</sub> (Minakshi, 2009; Pargoletti et al., 2016; M. Sun et al., 2014a; Y. Sun et al., 2016).

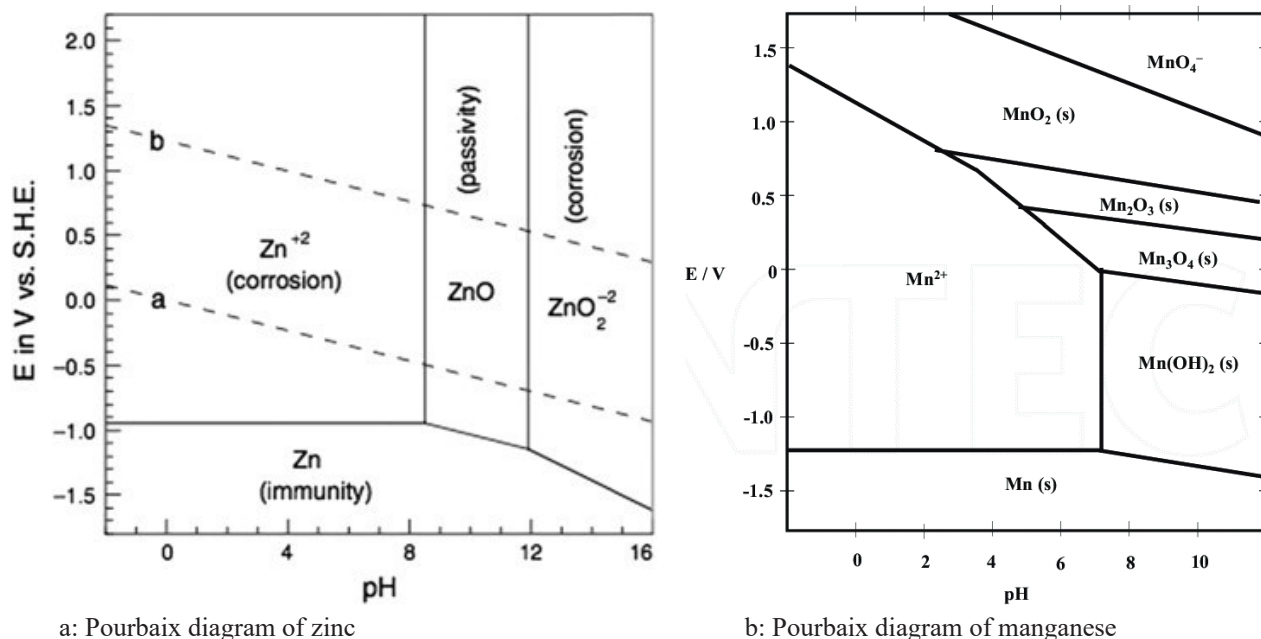


**Figure 7:** Equilibrium phases of zinc and manganese in aqueous media (McCafferty, 2010)

**Table 4:** Other example of cathodes for Zn-alkaline batteries

|   | Cathode | Half reactions & potential  | Cell potential |
|---|---------|---|----------------|
| 1 | NiOOH   | $\text{NiOOH}_{(s)} + 3\text{H}_2\text{O}_{(l)} + 2e^- \rightarrow \text{Ni(OH)}_{2(s)} + 2\text{OH}^-_{(aq)} + 0.50 \text{ V}$   | 1.65 V         |
| 2 | AgO     | $2\text{Ag}_{(s)} + 2\text{OH}^-_{(aq)} \rightarrow \text{Ag}_2\text{O}_{(s)} + \text{H}_2\text{O}_{(l)} + 2e^-$<br>$\text{Ag}_2\text{O}_{(s)} + 2\text{OH}^-_{(aq)} \rightarrow 2\text{AgO}_{(s)} + \text{H}_2\text{O}_{(l)} + 2e^-$ | 1.55V          |

### 3.2.2. Zinc-ion batteries

Environmental friendliness, low cost and safety continue to sustain the appeal of zinc as anode for aqueous battery system. The challenges associated with zinc-alkaline batteries operation at very high pH had compelled exploration of new chemistries at lower pH for zinc-aqueous battery. From its Pourbaix diagram, it is obvious that oxidation of zinc at  $\text{pH} < 8$  will give a soluble zinc cation. Therefore, in order to avoid a situation in Figure 3 (Nernst equation 1) where accumulation of zinc cation in solution leads to decrease of the cell potential, there must be a corresponding release of anion or cation uptake at the cathode. In other words, the potential cathode material must be able to undergo reduction with reversible release of anion or uptake of cation. Due to its small ionic radius, zinc cations can intercalation and de-intercalation inside layered structured materials. Several phases of manganese oxides have layered structures. So it is interesting that manganese oxide is a pioneer cathode

material that was investigated for zinc ion battery (Julien & Mauger, 2017; Mainar et al., 2016; Shin et al., 2019; D. Wang et al., 2019; J. Wang et al., 2019). X-ray diffraction (XRD) studies showed gradual transformation of tunnel-type  $\gamma\text{-MnO}_2$  into spinel-type  $\text{ZnMn}_2\text{O}_4$ , an evidence of intercalation of zinc cations into  $\gamma\text{-MnO}_2$  (N. Zhang et al., 2017). Thus, the redox reaction for the cell becomes:

**Table 5:** Cell reaction for Zn-ion battery

| Electrode | Electrode & cell reaction  |
|-----------|--|
| Anode     | $\text{Zn}_{(s)} \rightarrow \text{Zn}^{2+}_{(aq)} + 2e^-$                                   |
| Cathode   | $\text{Zn}^{2+}_{(aq)} + 2\text{MnO}_{2(s)} + 2e^- \rightarrow \text{ZnMn}_2\text{O}_{4(s)}$ |
| Overall   | $\text{Zn}_{(s)} + 2\text{MnO}_{2(s)} \rightleftharpoons \text{ZnMn}_2\text{O}_{4(s)}$       |

The overall cell reaction in Table 5 hides the fact that the reaction is not a solid-state reaction; aqueous zinc sulphate solution is usually employed as electrolyte. The pH of the electrolyte is expected to be  $\leq 7$ . At this pH, manganese oxides ( $\text{MnO}_2$ ,  $\text{Mn}_2\text{O}_3$ ) are prone to dissolution according to manganese Pourbaix diagram. A number of reports on zinc ion battery with manganese oxide cathode indicated cases of cathode dissolution. Addition of manganese sulphate to the electrolyte was found to suppress the cathode dissolution (Shin et al., 2019). This can be explained by Le-Chatelier's principle. However, the modified electrolyte alters the cathodic reaction and by extension the cell reaction as shown in Table 6.



**Table 6:** Cell reaction for Zn-ion battery in ZnSO<sub>4</sub>-MnSO<sub>4</sub> electrolyte

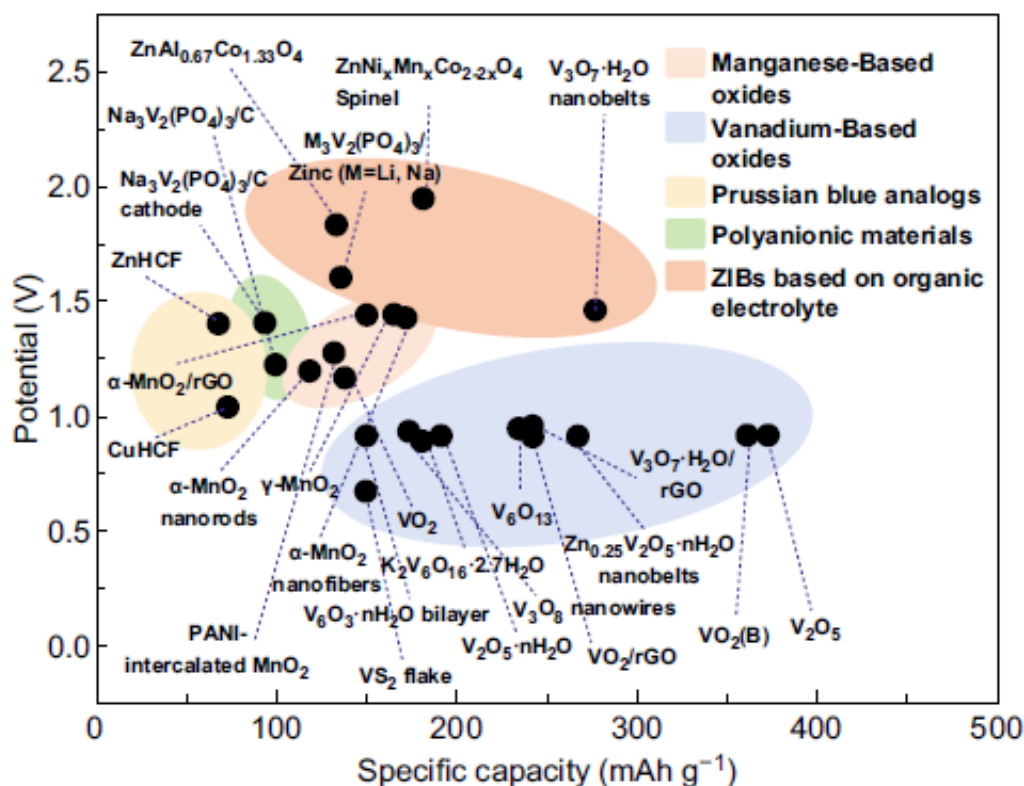
| Electrode | Electrode & cell reaction   |
|-----------|---|
| Anode     | $\text{Zn}_{(s)} \rightarrow \text{Zn}^{2+}_{(aq)} + 2e^{-}$  |
| Cathode   | $2\text{H}_2\text{O}_{(l)} \rightleftharpoons 2\text{H}^{+}_{(aq)} + 2\text{OH}^{-}_{(aq)}$<br>$2\text{MnO}_{2(s)} + 2\text{H}^{+}_{(aq)} + 2e^{-} \rightarrow 2\text{MnOOH}_{(s)}$<br>$\text{Zn}^{2+}_{(aq)} + 2\text{OH}^{-}_{(aq)} \rightarrow \text{Zn(OH)}_{2(s)}$ |
| Overall   | $\text{Zn}_{(s)} + 2\text{MnO}_{2(s)} + 2\text{H}_2\text{O}_{(l)} \rightleftharpoons \text{Zn(OH)}_{2(s)} + 2\text{MnOOH}_{(s)}$  |

**Table 7a:** Cell reaction for 2.432V Zn-ion battery (Yadav et al., 2019)

| Electrode | Electrode & cell reaction  | E°(V)<br>vs<br>Hg/<br>HgO |
|-----------|--|---------------------------|
| Anode     | $\text{Zn}_{(s)} + 4\text{OH}^{-}_{(aq)} \rightarrow \text{Zn(OH)}_4^{2-}_{(aq)} + 2e^{-}$   | -1.400                    |
| Cathode   | $\text{MnO}_{2(s)} + 4\text{H}^{+}_{(aq)} + 2e^{-} \rightarrow \text{Mn}^{2+}_{(aq)} + 2\text{H}_2\text{O}_{(l)}$                        | 1.132                     |
| Overall   | $\text{Zn}_{(s)} + \text{MnO}_{2(s)} + 2\text{H}_2\text{O}_{(l)} \rightleftharpoons \text{Zn(OH)}_4^{2-}_{(aq)} + \text{Mn}^{2+}_{(aq)}$ | 2.432                     |

**Table 7b:** Cell reaction for 2.4812 V Zn-ion battery (Yadav et al., 2019)

| Electrode | Electrode & cell reaction  | E°(V)<br>vs Hg/<br>HgO |
|-----------|--|------------------------|
| Anode     | $5\text{Zn}_{(s)} + 20\text{OH}^{-}_{(aq)} \rightarrow 5\text{Zn(OH)}_4^{2-}_{(aq)} + 10e^{-}$   | -1.400                 |
| Cathode   | $2\text{MnO}_4^{-}_{(aq)} + 16\text{H}^{+}_{(aq)} + 10e^{-} \rightarrow 2\text{Mn}^{2+}_{(aq)} + 8\text{H}_2\text{O}_{(l)}$                    | 1.412                  |
| Overall   | $5\text{Zn}_{(s)} + 2\text{MnO}_4^{-}_{(aq)} + 4\text{OH}^{-}_{(aq)} \rightleftharpoons 5\text{Zn(OH)}_4^{2-}_{(aq)} + 2\text{Mn}^{2+}_{(aq)}$ | 2.812                  |

**Figure 8:** Specific capacity vs discharge potential of some cathode materials for zinc ion batteries (Xu & Wang, 2019)

Proton uptake took place instead of zinc cation intercalation resulting in increase of the electrolyte pH which in turn leads to precipitation of the zinc cation in solution as hydroxide. Other metals that have variable oxidation states and stable oxide or phosphates phases in aqueous media had been investigated as cathodes for aqueous zinc ion batteries. Figure 8 gives an overview of electricity energy storage potentials of reported cathode materials for zinc ion battery as complied by Xu and Wang, (2019). As earlier mentioned, manganese oxides as well as vanadium and cobalt oxides have low electronic conductivity. Therefore, the cathodes are composites with significant amount of dead weights (inert conductive additive & binder).

Besides manganese oxides, vanadium species (oxides and phosphate) attracted more attention because of higher number of electron exchange of its oxides compared to those of manganese. Cobalt oxides are also interesting because of its reduction potential. Notably,  $V_2O_5$  based cathode was shown to give specific capacity double that of lead-acid battery. Also, the highest cell potentials (1.7–1.8 V) in Figure 8 were obtained using cobalt oxides based cathodes. Thus, it appears that aqueous zinc ion battery cannot match lead-acid battery in term of cell voltage by crossing 2.0V. However, there was a recent claim of 2.45 and 2.8 V aqueous Zn– $MnO_2$  batteries (Yadav et al., 2019). The cell diagram and cell reactions for the purported cells are shown in Figure 9 and Table 7 respectively. It is a divided cell containing two electrolytes, KOH gelled as anolyte and also serving as separator and  $H_2SO_4/KMnO_4$ - $MnSO_4$  as catholyte. Contrasting the reactions in Table 7 and the Pourbaix diagrams in Figure 7 shows that the claim of the authors appears to be predicated on moving to the right bottom corner of equilibrium phases of zinc (Figure 7a) and to the top left corner of equilibrium phases of manganese.

The cathodic reaction is the reverse of the typical method of commercial preparation  $MnO_2$  (electrolytic  $MnO_2$ ) that is suitable for battery application. The anodic and cathodic reaction products are aqueous ions. The separator the authors used is non-selective, hence, during cell operation, ions migrations across the separator will bring about irreversible reaction between the anodic and cathodic reaction product ions, as well as cause neutralisation reaction between the  $H_2SO_4$  and KOH that are hitherto on opposite side of the separator. Also, according to Figure 7b, the reverse of the cathodic reaction in Table 7b is not feasible in aqueous media. So, there are questions about reversibility of the cell and at best, the cell is only suitable as a primary cell. The few cycles reported by the authors may be attributed to the high concentration of  $H_2SO_4$  and KOH used. A

thermodynamically feasible means to cross the 2.0V threshold with Zn- $MnO_2$  couple is proposed in Table 8. Yet, a practical 2.0V Zn- $MnO_2$  battery is subject to fast reversible cathodic reaction and use of a cation exchange membrane as separator.

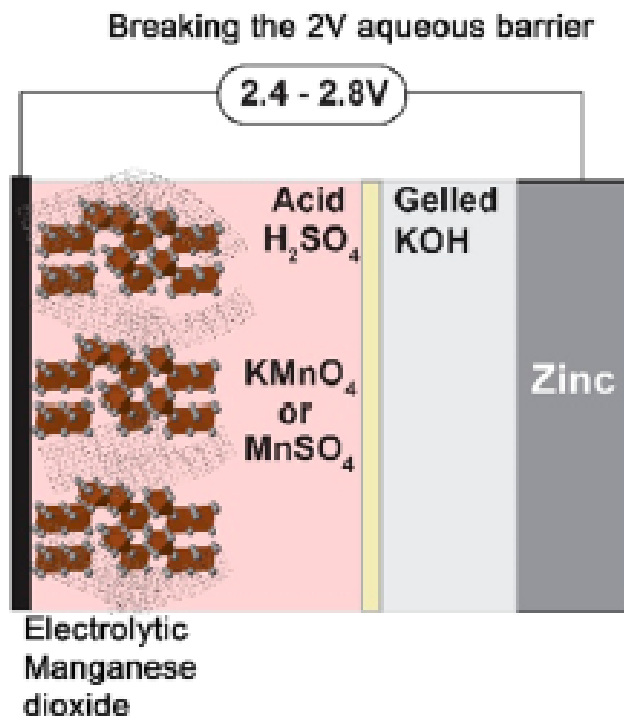


**Figure 9:** Cell diagram of a claimed 2.43 and 2.8V Zn-ion battery (Yadav et al., 2019)

**Table 8:** Proposed cell reaction towards > 2.0 V Zn-ion battery

| Electrode | Electrode & cell reaction   | $E^\circ(V)$<br>vs Hg/<br>HgO |
|-----------|---|-------------------------------|
| Anode     | $3Zn_{(s)} + 12OH^-_{(aq)} \rightleftharpoons 3Zn(OH)_4^{2-} + 6e^-$                          | -1.400                        |
| Cathode   | $2MnO_4^- + 4H_2O + 6e^- \rightleftharpoons 2MnO_2 + 8OH^-$<br>$(aq)(l)$                      | 1.000                         |
| Overall   | $3Zn_{(s)} + 2MnO_4^- + 4OH^-_{(aq)} \rightleftharpoons 3Zn(OH)_4^{2-} + 2MnO_2$<br>$(aq)(s)$ | 2.400                         |

Besides the need for inert conducting additive and the attendant composite stability challenges, the constraint of equilibrium phases of metal oxide in aqueous media is palpable in any aqueous zinc ion battery design attempt. There are efforts at exploring for cathode materials that do suffer these limitations. Organic materials, especially conducting polymers are prime candidates because of their higher conductivities due to their extensive  $\pi$ -electron conjugated systems. Polyaniline (PANi) in particular is of peculiar interest because of its redox property, low

cost and simple method of synthesis. With four aniline units per two electron two proton redox reaction (Figure 10), and the cell reaction (Table 9) for Zn-PANi battery is similar to that in Table 6. In a Zn/Zn<sup>2+</sup>, NH<sub>4</sub><sup>+</sup>/PANi cell, slightly alkaline medium was used so as to prevent corrosion of zinc (Li et al., 2008). PANi usually form non-conducting leuco-emeraldine base at alkaline pH, but good electrochemical activity was reportedly at pH 5.5 because of large buffer capacity of the electrolyte. A self-doped PANi prepared via co-polymerisation of aniline and 3-aminobenzoic displayed enhanced cycling stability in the ZnCl<sub>2</sub>-NH<sub>4</sub>Cl electrolyte. Even longer cycle life in an unbuffered ZnSO<sub>4</sub> solution was obtained using self-doped PANi prepared from aniline and metanilic acid copolymer (Shi et al., 2018; Rahmanifar et al., 2002). The improved cycle life span obtained with self-doping is at the expense of decrease of theoretical specific storage capacity.

**Table 9:** Cell reaction for PANi - Zn-ion battery in ZnSO<sub>4</sub> electrolyte

| Electrode | Electrode & cell reaction   | E°(V)   |
|-----------|---|---------|
| Anode     | $\text{Zn}_{(s)} \rightarrow \text{Zn}^{2+}_{(aq)} + 2e^-$  | -0.7618 |
| Cathode   | $2\text{H}_2\text{O}_{(l)} \rightleftharpoons 2\text{H}^{+}_{(aq)} + 2\text{OH}^{-}_{(aq)}$<br>$\text{PANi}_{(s)} + 2\text{H}^{+}_{(aq)} + 2e^- \rightarrow \text{PANi-H}_{2(s)}$<br>$\text{Zn}^{2+}_{(aq)} + 2\text{OH}^{-}_{(aq)} \rightarrow \text{Zn(OH)}_{2(s)}$ | 0.6000  |
| Overall   | $\text{Zn}_{(s)} + \text{PANi}_{(s)} + 2\text{H}_2\text{O}_{(l)} \rightleftharpoons \text{Zn(OH)}_{2(s)} + \text{PANi-H}_{2(s)}$  | 1.3618  |

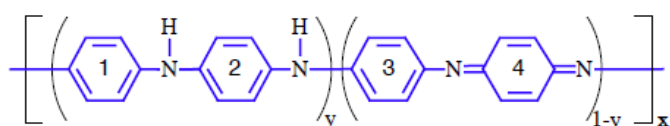


**Figure 10:** The asymmetric chemical structure of Polyaniline (PANi) (Magnuson et al., 1999)

**Table 10:** Theoretical specific capacity of external proton doped and self-doped PANi

| Polyaniline                  | Theoretical specific capacity (mAhg <sup>-1</sup> ) |
|------------------------------|---|
| H <sup>+</sup> doped         | 148.1   |
| COOH self-doped              | 118.1   |
| SO <sub>3</sub> H self-doped | 101.9   |

With specific storage capacities lower than PbO<sub>2</sub> and low cell voltage PANi seems unattractive as a cathode material for commercial aqueous battery. Since PANi has very similar redox chemistry with quinones, in a similar

motivation to achieve increased cell voltage, Cai et al., (2019) adopted a divided cell design using bifunctional partition to obtain Zn-quinone battery that has 2.02 cell voltage (Figure 11). The cell reaction is very similar to that of Zn-PANi but with difference of maintaining high pH at anodic chamber and elaboration of water splitting with the use of bifunctional membrane.

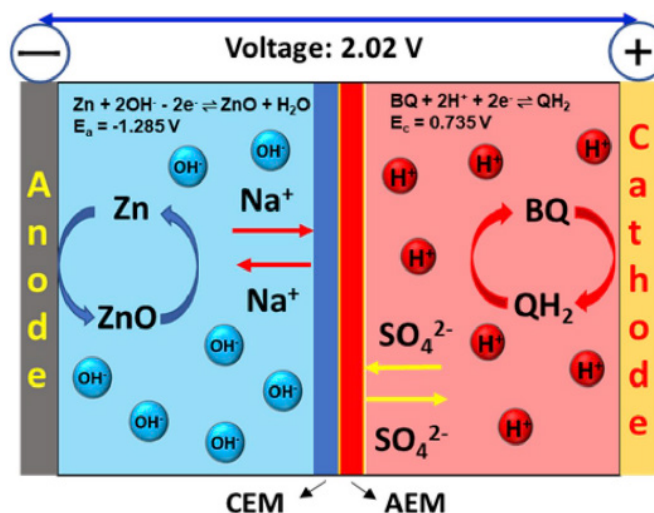


**Figure 11:** 2.02 V Zn-quinone battery (Cai et al., 2019)

**Table 9:** Cell reaction for Zn-Quinone battery using dual base-acid media with the aid of bifunctional membrane

| Electrode | Electrode & cell reaction  | E°(V)   |
|-----------|--|---------|
| Anode     | $\text{Zn}_{(s)} + 2\text{OH}^{-}_{(aq)} \rightarrow \text{ZnO}_{(s)} + \text{H}_2\text{O}_{(l)} + 2e^-$   | -1.28 V |
| Cathode   | $2\text{H}_2\text{O}_{(l)} \rightleftharpoons 2\text{H}^{+}_{(aq)} + 2\text{OH}^{-}_{(aq)}$<br>$\text{Q}_{(aq)} + 2\text{H}^{+}_{(aq)} + 2e^- \rightarrow \text{QH}_{2(aq)}$ | 0.740   |
| Overall   | $\text{Zn}_{(s)} + \text{Q}_{(aq)} + 2\text{H}_2\text{O}_{(l)} \rightleftharpoons \text{ZnO}_{(s)} + \text{QH}_{2(aq)}$  | 2.02    |

In a related development, a PANi-MnO<sub>2</sub> hybrid was investigated as cathode material for zinc ion battery. The hybrid cathode displayed 280 mAhg<sup>-1</sup> specific capacity and high cycle life span. The storage capacity obtained was about the theoretical value for MnO<sub>2</sub> while the improve cycle lifespan was attributed to PANi acting as binder that fortifies MnO<sub>2</sub> minimised phase changes associated with the redox cycle on the MnO<sub>2</sub> nanostructure (J. Huang et al., 2018). This role as a conducting and redox active binder can rekindle interest in PANi as useful material for reducing dead weights of composite cathodes preparations provided the cathodic reaction synchronise with that of PANi. The synergy of the conducting backbone of PANi and a covalently linked redox active pendant organic groups (such quinones) as demonstrated by Sjödin and co-workers

for polypyrrole and PEDOT (Bahceci & Esat, 2013; H. Huang et al., 2013; Sterby et al., 2017) offers another plausible strategy to expand the cathode utility of PANi.

So far, it is evidently clear that water plays a central role in aqueous battery systems. It is the medium of ion migrations to the electrodes. Water is cheap, abundant and non-flammable which minimises chances of combustion accident. Its high dielectric constant, high boiling point, and low viscosity are desirable combination of properties that promote high ionic conductivity. Water is also an active participant in electrode reactions. Aqueous batteries composed of strictly metal/metal ion electrodes, the potential window of stability region of water is a ubiquitous constraint on obtainable cell voltage (Tang et al., 2019). The constraint can be relaxed when one or the two metal/metal ion electrodes are replaced with those whose electrode reaction involves direct or indirect water splitting. Therefore, water-splitting reaction is part of the energy storage. This provides means to widen obtainable cell voltage within the limit of avoiding extensive hydrogen and oxygen evolution. Yet, the constraint is only relaxed not eliminated. Stability of conductors or current collectors in aqueous electrolytes also puts limitations on materials selection for aqueous batteries. Thus, use of non-aqueous electrolyte system helps to side step the limitations but with new challenges.

#### 4. Non-aqueous battery systems

The quest to find alternative to water in order to circumvent its limitation for battery design must reconcile two contrasting criteria (Liu et al., 2020). The potential candidates must be inert to the electrode reactions, and must possess the desirable solvent properties: high dielectric constant, high boiling point, and low viscosity. The class of solvents that come close to meeting the criteria is known as *polar aprotic solvents*. These solvents are polar compounds/solvents (i.e. they have permanent non-zero dipole moment), and contain no acidic hydrogen atoms (i.e. contain no hydrogen bond donor). Absence of acidic hydrogen is critical to inert behaviour while dipole moment is essential to exhibiting polar character. The prospective alternative solvents must possess excellent ability to dissolve ionic compounds like water (Frk et al., 2013). Although dipole moment is an essential molecular property, dielectric constant as a bulk property, is a more useful descriptor of ability of a solvent to dissolve ionic compounds. Table 10 shows some properties of some polar aprotic solvents. Cyclic ester solvents (ethylene and propylene carbonate) are close a match to water in terms of dielectric constant. This explains why they are

among the most explored for constituting electrolytes for non-aqueous battery systems.

**Table 10:** Solvent properties of some polar aprotic solvents (Xu, 2004)

| Solvent             | Dipole moment (D) | Dielectric constant | Boiling point (°C) | Density (g/mL) |
|---------------------|-------------------|---------------------|--------------------|----------------|
| Water               | 1.85              | 80                  | 100                | 1.000          |
| Ethyl acetate       | 1.78              | 6.0                 | 77                 | 0.894          |
| Tetrahydrofuran     | 1.75              | 7.5                 | 66                 | 0.886          |
| Dichloromethane     | 1.60              | 9.1                 | 40                 | 1.326          |
| Acetone             | 2.88              | 21                  | 56                 | 0.786          |
| N-methylpyrrolidone | 4.10              | 33                  | 202                | 1.028          |
| Dimethylformamide   | 3.82              | 38                  | 153                | 0.944          |
| Acetonitrile        | 3.92              | 37                  | 82                 | 0.786          |
| Dimethyl sulfoxide  | 3.96              | 47                  | 189                | 1.092          |
| Propylene carbonate | 4.90              | 64                  | 242                | 1.205          |
| Ethylene carbonate  | 4.90              | 89.78               | 243                | 1.321          |

##### 4.1. Non-aqueous metal ion batteries

After identifying prospective alternatives to water, next is to choose or select electrodes (cathode and anode) that will constitute the battery. It makes no economic sense to employ non-aqueous electrolyte for zinc or lead based batteries. The electrochemical window of zinc and lead electrodes are well accommodated in aqueous electrolytes. Elements that have more negative reduction potential than zinc (-0.76V) will give higher cell voltage and higher specific capacity that will justify the electrolyte cost. The elements that meet this demand are Li, Na, Mg & Al with theoretical specific capacities 3862, 1165.8, 2205, 2980mAhg<sup>-1</sup> respectively. With the exception of Al, the chemistry of these elements are characterized by extreme reactivity with air and water. With no Pourbaix diagrams (as available for aqueous systems), development of electrodes of these metals was uncharted water; their electro-metallurgy was the only guide. With the inert requirement of the solvent, to obtain metal/metal ion electrode (e.g.  $\text{Li} \rightleftharpoons \text{Li}^+ + \text{e}^-$ ), the metal salt dissolved in the solvent will constitute the electrolyte. The anode will consist of the metal in contact with a non-aqueous solution of its salt. The corresponding cathode reaction also must avoid air. In order to maximise obtainable cell voltage, the complementary cathode reaction should have high positive reduction potential. Also to preserve the cell/battery stoichiometry and reversibility, the cathode



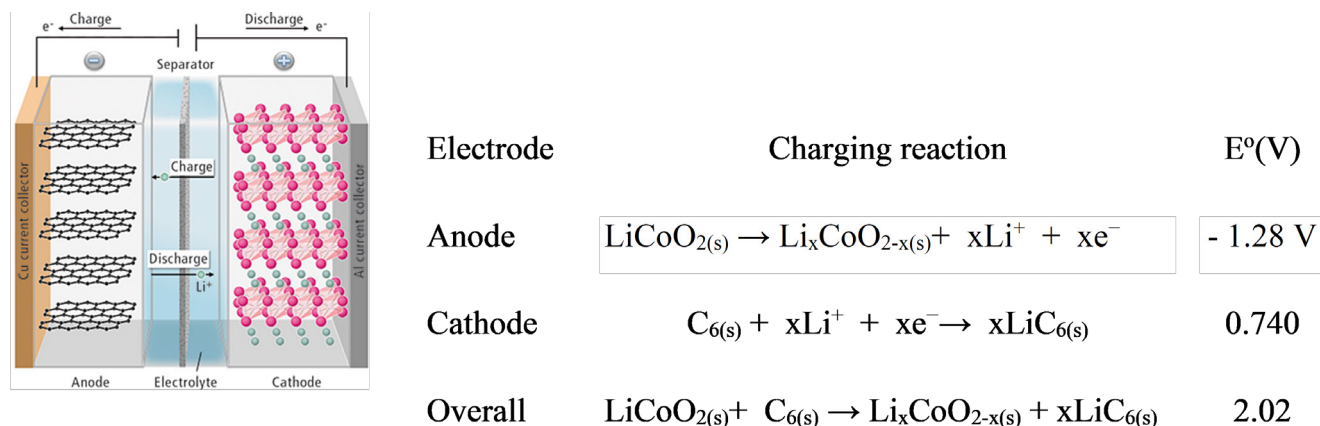


**Figure 12:** Schematic description of a typical lithium ion battery and the cell reaction (Galashev & Ivanichkina, 2018)

material must possess excellent ability to intercalate and de-intercalate the metal ion. Therefore, the cell chemistry for non-aqueous battery systems appears simpler because it is devoid of the participation of the solvent. However, the electrode development is complicated because of the requirement of air and water free conditions. The electrode development requirements and challenges are different for each metal. Because of their higher theoretical specific capacities, we will discuss in brief detail lithium and aluminium in the next section.

#### 4.2. Lithium battery

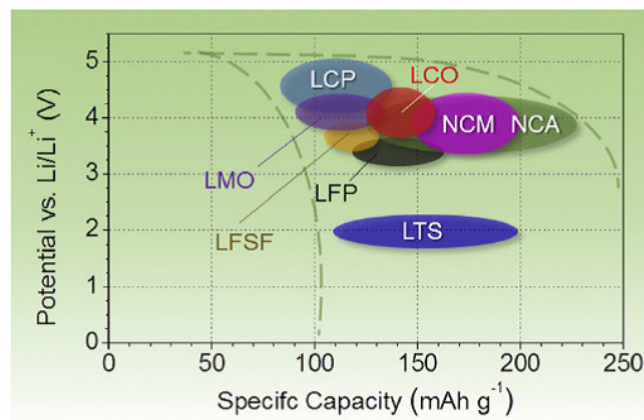
Lithium ion battery is a prime success story among non-aqueous battery systems. Its current market share is only second to lead-acid battery. It is pivotal to the small electronics and portable computer revolution. It is also the leading candidate for electric vehicles and many portable applications. Although the key demands for non-aqueous battery chemistry is established, the development of practical lithium battery is a long tortuous journey. The impact of lithium ion battery is phenomena. It is no wonder that John B. Goodenough, M. Stanley Whittingham, and Akira Yoshino were jointly awarded the 2019 Chemistry Nobel Prize for the landmark contributions towards development of a practical lithium battery. Specific contributions of each of them are well documented in the literature and specific summary captured in scientific background on the Nobel Prize in Chemistry 2019 (The Royal Swedish Academy Of Sciences, 2019). Readers are encouraged to consult the documents for details. We will only examine the chemistries of the current practical lithium ion battery cell configuration.

The essential feature of the current configuration of the first commercial lithium ion battery is shown in Figure 12. The cell is often referred to as ‘rocking-chair’ design because lithium ion de-intercalate from the cathode and migrates towards and intercalate in between the layers of the anode during charging. The reverse takes place during discharging. Although, dielectric constant ethylene carbonate was greater than that of propylene carbonate, ethylene carbonate is a solid at ambient temperature but propylene carbonate is a liquid, so propylene carbonate was chosen, and  $\text{LiPF}_6$  dissolve in propylene carbonate was used as electrolyte. It was impractical to use metallic lithium as anode because its reactivity with air and moisture. Also uncontrollable dendrites growth that could short circuit the cell remained unresolved with metallic lithium anode. Lithium-graphite intercalation compounds,  $\text{Li}_x\text{C}_6$  (where  $0 \leq x \leq 1$ ), had been earlier discovered and studied. Because graphite is cheap and abundant, it ought to be a natural choice as anode material. However, propylene carbonate and graphite were found incompatible. It was found that during discharging, propylene carbonate decomposes on the surface of the graphite. The decomposition product formed an electronically insulating layer and its accumulation results in passivation of the graphite. However, reversible intercalation and de-intercalation was achieved when conducting carbon materials produced from petroleum coke was used as anode. Conducting carbon produced from petroleum coke was the first practical anode material. Later, it was discovered that when ethylene carbonate/propylene carbonate co-solvent was used the decomposition product layer formed an ionically conducting and mechanically robust interphase. This was termed *solid electrolyte interphase*.

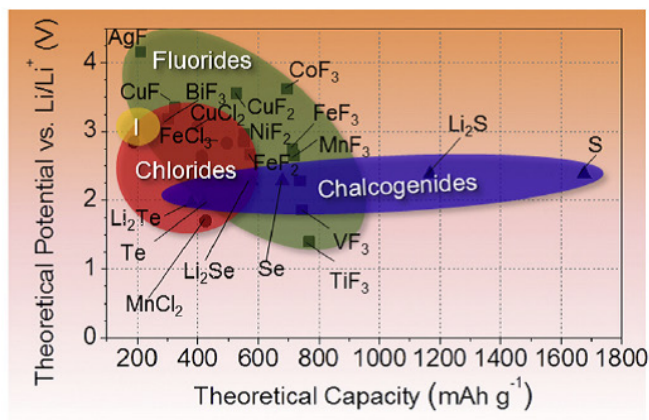
(SEI) (Gauthier et al., 2015; Peled, 1979). Electronic insulation of the SEI prevents further direct contact between lithium atom and propylene (solvent), thereby protecting the graphite from complete passivation. Its ionic conductivity preserves the reversibility of the lithium intercalation and de-intercalation into the graphite.  $\text{LiCoO}_2$  is the cathode material in the first commercial lithium ion battery. It consists of  $\text{CoO}_2$  layers with van der Waals gaps that accommodate lithium ions. Oxidation state of cobalt in  $\text{LiCoO}_2$  is +3, during charging oxidation state of cobalt increases to +4 and lithium ions diffuse out of the layers into the electrolyte and migrate to the anode. The reverse takes place during discharge. A separator usually a micro-porous film of polypropylene prevents short-circuiting of the cell. Thus, the requirement to make a non-aqueous

battery was met and the first practical or commercial lithium ion was born. It formed the template for further improvements on lithium ion battery and development of other non-aqueous metal ion batteries.

The birth of lithium ion battery had demonstrated the possibility of achieving higher cell voltage in non-aqueous system. The rocking chair chemistry also favours constant discharge voltage; the specific capacity achieved is only a small fraction of the theoretical capacity of lithium. This is because use of metallic lithium is impractical; the obtainable capacity depends on lithium ion intercalation capacity of the cathode (Yoshino, 2012). Moreover, a working cathode is a composite (transition metal oxide, conductive carbon & binder). Reported ranges of energy storage capacities of some leading cathode materials of commercial lithium

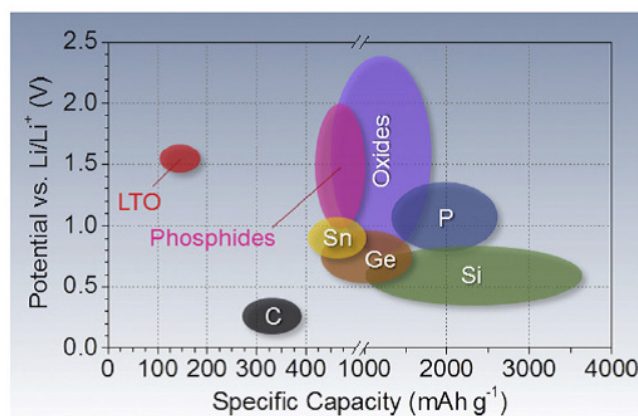


a. Intercalation cathodes

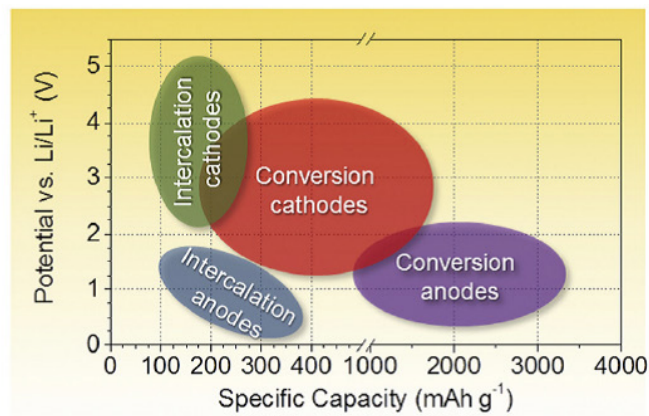


b. Conversion cathodes

Figure 13: Average storage capacities of some intercalation based cathodes (Nitta et al., 2015)



a. Conversion based anode



b. Cathode-anode combinations for Lithium battery

Figure 14: Ranges of energy storage capacities of conversion based cathodes and cathode-anode combinations for Lithium battery (Nitta et al., 2015)

ion batteries are shown in Figure 13a. There are other transition metal analogues of  $\text{LiCoO}_2$  designated as LCO. Other designations are: LMO- $\text{LiMnO}_2$ , NCM- $\text{LiNi}_x\text{Co}_y\text{Mn}_{1-x-y}\text{O}_2$ , NCA- $\text{LiNi}_x\text{Co}_y\text{Al}_{1-x-y}\text{O}_2$ , LPO- $\text{LiCoPO}_4$ , LFP- $\text{LiFePO}_4$ , LFSF- $\text{LiFeSO}_4\text{F}$  & LTS- $\text{LiTiS}_2$  (Nitta et al., 2015). They are intercalation based cathode materials. They have the advantages of high number of cycle spans (5,000–10,000).

Low specific capacities had motivated the investigations of conversion chemistries that will afford high lithium ion uptake capacity. This is only achievable with low molecular mass material that can undergo multi-electron redox reaction with lithium ions. As shown in Figure 13b, the material that satisfies this requirement is sulphur. But making a functional sulphur cathode is not trivial. To start with, sulphur is an insulator. Redox reaction between sulphur and lithium ion is complex and associated with large volume change with attendant detrimental effect on the structural integrity of the resulting cathode. The physical solution to the high volume change is minimised volume/surface area ratio. This translates into using sulphur particle size as small as possible. Next, is to devise a way to hold the sulphur particles and conductive additive together. Cui and co-workers approach this challenge by exploiting nanotechnology techniques to devise composites of sulphur nanostructures and conducting polymers (Chang et al., 2018; Li et al., 2013; Seh et al., 2013). The composite cathodes obtained displayed high cycle life. Recently, used high-modulus binder such as carboxymethylcellulose (CMC) was reported. Carboxylic acid group functionalized CMC enables the formation of mechanically strong sulphur cathode. The use of carboxylic acid group rich CMC produced expansion-tolerant architectures that allows for stable cycling of the cathode even with ultra-high sulphur loading.

High capacity cathode is only half-way the requirement to achieve high cell/battery. It has to be complemented by a high capacity anode. The maximum obtainable specific capacity of graphite anode is  $\sim 370 \text{ mAhg}^{-1}$ . In order to complement improved cathode storage capacity, conversion chemistries were investigated for lithium atom storage. Figure 14a shows average reported energy storage capacities of anode material for lithium ion battery. Only LTO ( $\text{Li}_2\text{TiO}_3$ ) has lower specific capacity than graphite (C). It has advantage of being faster to charge than others in the chart. The material showing highest specific capacities is silicon. Although silicon is relatively more conductive than sulphur, it suffers the same volume expansion problem. Cui and co-workers made significant contributions towards solutions to this

problem. They devise several silicon nanostructures to prevent damaging volume change. They also use self-healing polymers as binder for the resulting composite material (Munaoka et al., 2018; C. Wang et al., 2013). The strategies produced stable and high cycle life span anodes. Figure 14b depicts the obtainable energy storage capacities of anode-cathode combinations for lithium ion battery. The cell capacity of intercalation based lithium ion battery is limited by the specific capacity of cathodes which appears to have stagnate at  $\sim 230\text{--}370 \text{ mAhg}^{-1}$ . The conversion electrodes based lithium ion battery is the most promising future lithium ion battery with 1000-1500 specific capacity. Yet, the obtainable capacity is still less than half-theoretical specific storage capacity of lithium.

Other significant development on lithium ion battery is replacement of liquid electrolyte with polymer electrolytes. Solid polymer electrolyte intended to improve safety of lithium ion battery by eliminating incidence of electrolyte leakage and flammability of liquid electrolyte. With solid polymer electrolyte serving as separator, net weight of lithium-polymer battery is expected to be smaller than that liquid electrolyte lithium battery. This would lead to higher specific energy suitability for applications such mobile devices where weight is a critical desirable feature. Initially, solid polymer electrolytes are produced by solid-solid solution of lithium salt and polymer blends from poly(ethylene oxide) (PEO) and one or more of poly(acrylonitrile) (PAN), poly(methyl methacrylate) (PMMA) & poly(vinylidene fluoride) (PVdF). The resulting solid electrolytes often exhibit low ionic conductivities. In recent times in order to match conductivities of liquid electrolytes, customised polymer designs are been reported (Shaibani et al., 2020). Some of the new polymers are zwitterionic (containing cationic and anionic on or covalently bonded to polymer backbone). Some other have solvent group (e.g. ethylene carbonate) on polymer backbone (Keith & Ganesan, 2020; Lu et al., 2017; Tiyaipiboonchaiya et al., 2004). The new polymers enhance lithium salt dissociation without competing mobile ionic species.

Since the market success of the rocking chair chemistry configuration lithium ion battery has witnessed significant improvements on the intercalation architecture. Currently, improvements on specific capacity that is based on the intercalations architecture appears very close to saturation point. Quest for big leap in specific capacity has necessitated a departure from the intercalation chemistry to conversion-type chemistry. This departure from the familiar features (no bond breaking, no movement and little or no change of volume & structure) of the intercalation electrodes will



have to be sacrificed in the quest for increase of specific capacity. The embrace of the conversion-type chemistry comes with the challenges, which include: reversibility of electrode processes, breaking and formation of bonds, electrode/electrolyte contacts, volume & structural changes. No doubt, lithium battery is ubiquitous in laptop, mobile and other portable applications, it is also the candidate in some electric vehicle brands such as Tesla, and it has not made in-road into grid-scale application due largely to its high cost relative to lead-acid battery.

#### 4.3. Aluminium battery

Aluminium is next to lithium among prospective metals that are desirable for non-aqueous battery. Aluminium's shortfall in terms of reduction (about 1.4V lower compared to lithium) was partly made up for by three electron exchange per aluminium atom (Hong et al., 2019). Therefore, its theoretical specific capacity is a motivation for quest to devise aluminium battery. Coincidentally aluminium extraction industry has a long history of large electricity consumption (Leisegang et al., 2019). Most industrial primary aluminium production use Hall-Héroult electrolysis cells (Kvande, 2010). They used alumina ( $\text{Al}_2\text{O}_3$ ) dissolved in molten cryolite ( $\text{Na}_3\text{AlF}_6$ ) at about 960 °C. This operating temperature of Hall-Héroult electrolysis cell is a far cry from what is desirable for a battery. Thus, it is necessary that the chemistry of aluminium production be adapted or modified to make it suitable or devise new one for electricity storage applications. The cell reaction of Hall-Héroult electrolysis is represented in Table 11.

**Table 11:** Cell reaction of Hall-Héroult electrolysis

|                          |   |
|--------------------------|---|
| Dissociation             | $2\text{Al}_2\text{O}_{3(\text{melt})} \rightleftharpoons 4\text{Al}_{(\text{melt})}^{3+} + 6\text{O}_{(\text{melt})}^{2-}$ |
| Cathodic half – reaction | $4\text{Al}_{(\text{melt})}^{3+} + 12\text{e}^- \rightarrow 4\text{Al}_{(\text{s})}$  |
| Anodic half – reaction   | $6\text{O}_{(\text{melt})}^{2-} + 3\text{C}_{(\text{s})} \rightarrow 3\text{CO}_{2(\text{g})} + 12\text{e}^-$               |
| Net reaction             | $2\text{Al}_2\text{O}_{3(\text{l})} + 3\text{C} \rightarrow 4\text{Al}_{(\text{s})} + 3\text{CO}_{2(\text{g})}$             |

For electrolysis to take place, ions must migrate to the electrodes where oxidation and reduction will take place. The first step of the process is dissociation of alumina. Melting point of alumina is about 2,072 °C. This is extremely high. Lower temperature of 960 °C is obtained with cryolite-alumina eutectic mixture. The melting temperature is realised by force high current through the mixture (this step of critical aspect of the Hall-Héroult electrolysis consumes substantial amount

of electricity). Once the alumina melts the ions migrates to the respective electrode where aluminium is deposited at the cathode and oxide ion is discharged as  $\text{CO}_2$  at the anode (the graphite anode is sacrificed). Theoretically, 1.22 gram of carbon dioxide should be generated per gram of aluminium deposited. In practice, the amount of  $\text{CO}_2$  generated is far greater.  $\text{CO}_2$  emission of aluminium extraction had been a concern over the years in the light of its greenhouse effect and attendant global warming and climate change. There are advocacy for adoption of less energy intensive and  $\text{CO}_2$  emission for aluminium production. Key aspects of the Hall-Héroult electrolysis that must be changed to make it suitable for battery chemistry are:

- electrolyte system that will allow reversible electro-deposition of aluminium at ambient temperature; and
- replacing the terminal or sacrificial anodic reactions with a reversible one.

##### 4.3.1. Electrolytes for aluminium battery

For informed solutions to the stated problems above, it is imperative to identify the origin of the problem. The data of lattice energies of crystal of binary aluminium compounds and their respective melting points clearly shows that aluminium cation is highly oxophilic (Table 12). The alumina lattice energy is so strong that it cannot be solvated by common solvents or molten salts except few fluorides ( $\text{CaF}_2$ ,  $\text{AlF}_3$ ). Thus, any electrolyte system and electrodes that will enable ambient temperature reversible electro-deposition of aluminium must exclude presence of active oxygen species.

**Table 12:** Lattice energies and melting points of some aluminium compounds

| Anion                                 | F <sup>-</sup> | Cl <sup>-</sup> | Br <sup>-</sup> | I <sup>-</sup> | O <sup>2-</sup> |
|---------------------------------------|----------------|-----------------|-----------------|----------------|-----------------|
| Lattice energy (kJmol <sup>-1</sup> ) | 5215           | 5492            | 5361            | 5218           | 15916           |
| Melting point                         | 1,290          | 192.6           | 97.5            | 188            | 2,072           |

##### 4.3.2. $\text{AlCl}_3$ -halide salt melts

At first glance, the data in Table 12 suggests that bromide appears the likely choice aluminium salt for electrolyte preparation, but aluminium bromide is very reactive and more expensive than chloride. Also chloride salts are generally more thermally stable than bromide salts. For electricity storage applications chloride is more attractive from cost perspective. Before battery application intentions reported alternative electrolytes



to Hall-Héroult electrolysis for aluminium electro-deposition involved use of  $\text{AlX}_3$  (Cl, Br) dissolved in alkali or organic ammonium halides melts (e.g. 66–20–14 wt%  $\text{AlCl}_3$ – $\text{NaCl}$ – $\text{KCl}$  melts at 115°C) (Jafarian et al., 2006).  $2\text{AlCl}_4^- \rightleftharpoons \text{Al}_2\text{Cl}_7^- + \text{Cl}^-$  equilibrium exists in the salt melts. With the halide salts melts, two aluminium electro-deposition reactions were recognised:  $4\text{Al}_2\text{Cl}_7^- + 3\text{e}^- \rightarrow \text{Al} + 7\text{AlCl}_4^-$  in acidic melt, and  $\text{AlCl}_4^- + 3\text{e}^- \rightarrow \text{Al} + 4\text{Cl}^-$  in basic melt. The acid-base behaviour depends on molar ratio  $\text{AlCl}_3$ /alkali or organic ammonium halide in the melt. With organic ammonium halides especially imidazolium cation recently, the resulting salt melts are liquids at room temperature and aluminium electro-deposition proceeds through acidic melt (i.e.,  $\text{AlCl}_3$ /imidazoliumcation, usually 2:1 - 3:2) (Böttcher et al., 2019; Kitada et al., 2016; Lai, 1989; Tu et al., 2017; Zein El Abedin et al., 2006)

$\text{AlCl}_3$  dissolved in aromatic hydrocarbon had also been found as electrolyte for aluminium electro-deposition. In a  $\text{AlBr}_3$ -alkylbenzene electrolyte, aluminium electro-deposition proceeds was found to proceed via:  $2[\text{AlBr}_2(\text{C}_6\text{H}_5\text{C}_2\text{H}_5)_n]^+ + 3\text{e}^- \rightarrow \text{Al} + \text{AlBr}_4^- + 2n(\text{C}_6\text{H}_5\text{C}_2\text{H}_5)$ . Weakly basic aromatic hydrocarbon such as benzene and toluene formed dimeric  $\pi$ -complex ( $\text{Al}_2\text{X}_6 + \text{ArH} \rightarrow [\text{Al}_2\text{X}_5\text{ArH}]^+ + \text{X}^-$ ) in solution while strong basic aromatic hydrocarbon such trialkylbenzenes formed monomeric  $\pi$ -complex ( $\text{Al}_2\text{X}_6 + \text{ArH} \rightarrow [\text{AlX}_2\text{ArH}]^+ + [\text{AlX}_4]^-$ ) (Capuano, 1991). Recently, similar behaviour as in  $\text{AlBr}_3$ -alkylbenzene electrolyte had been reported for  $\text{AlCl}_3$ -urea,  $\text{AlCl}_3$ -amide,  $\text{AlCl}_3$ -dipropylsulfide,  $\text{AlCl}_3$ -glyme, and  $\text{AlCl}_3$ -4-propylpyridine electrolytes ( $\text{Al}_2\text{Cl}_6 + \text{solvent} \rightarrow [\text{AlCl}_2(\text{solvent})_n]^+ [\text{AlCl}_4]^-$ ) (Angell et al., 2017; Bian et al., 2018; Fang et al., 2015; Kitada et al., 2016; M. Li et al., 2017). The prospective cell reaction of the resulting aluminium battery is presented in Table 13.

**Table 13:** Prospective cell reaction of for  $\text{AlCl}_3$ -halide salt melts electrolytes Al-ion batteries

|                          |   |
|--------------------------|---|
| Anodic half – reaction   | $\text{Al} + 7\text{AlCl}_4^- \rightarrow 4\text{Al}_2\text{Cl}_7^- + 3\text{e}^-$<br>or<br>$\text{Al} + \text{AlCl}_4^- + 2n(\text{Urea}) \rightarrow 2[\text{AlCl}_2(\text{Urea})_n]^+ + 3\text{e}^-$   |
| Cathodic half - reaction | $3\text{C}_x^+ + 3\text{e}^- + 3\text{AlCl}_4^- \rightarrow 3\text{C}_x \cdot \text{AlCl}_4^-$  |
| Overall - reaction       | $\text{Al} + 10\text{AlCl}_4^- + 3\text{C}_x^+ \rightarrow 4\text{Al}_2\text{Cl}_7^- + 3\text{C}_x \cdot [\text{AlCl}_4]^-$<br>or<br>$\text{Al} + 4\text{AlCl}_4^- + 2n(\text{Urea}) + 3\text{C}_x^+ \rightarrow 2[\text{AlCl}_2(\text{Urea})_n]^+ + 3\text{C}_x \cdot [\text{AlCl}_4]^-$ |

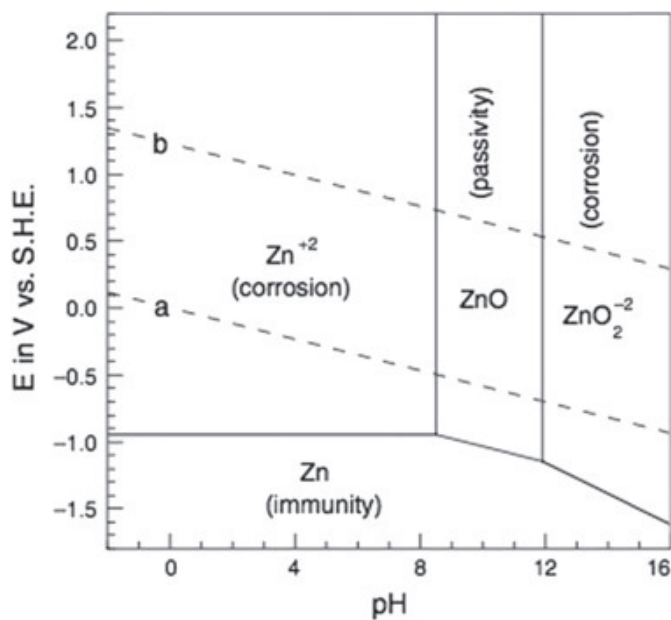
A very startling contrast between the cell reaction of Li-ion battery and  $\text{AlCl}_3$ -halide salt melt Al-ion batteries is the stack involvement of the electrolyte in the cell reaction. As rightly cautioned recently (Shi et al., 2019), this fact was overlooked in most reported studies on Al battery with salt melt electrolytes. The implication of this is that cell discharge voltage will depend strongly on the electrolyte. Going from high temperature chemistry (molten  $\text{Al}_2\text{O}_3$  at 960 °C) to ambient temperature chemistry ( $\text{AlCl}_3$ -halide salt melts), this radical change in possibility of reversible electro-deposition of aluminium motivated the exploration of  $\text{AlCl}_3$ -halide salt melts electrolytes for aluminium battery design.

The complementary cathode reaction to the anodic reactions in  $\text{AlCl}_3$ -halide salt melt electrolytes is quite different from that of lithium ion battery. Here the cathode has to intercalate  $[\text{AlCl}_4]^-$  anion, which requires that the cathode becomes electrophilic upon reduction. Moreover, prospective cathode material has to be resistant to chloride corrosion and Friedel-Crafts reactions. There are very few materials that are resistant to chloride corrosion. High capacity cathode materials used in zinc and lithium ion batteries displayed low stability in the  $\text{AlCl}_3$ -halide salt melts electrolyte. Only graphite in its natural or modified appears to meet the stability requirement from which high cycle life span were reported albeit with low specific capacities. The  $\text{C}_x$  in Table 13 represents graphite or other forms of layered carbon material, and x is number of carbon atoms per intercalated anion, for instance,  $x = 30$  based on 75  $\text{mAhg}^{-1}$  capacity) (Shi et al., 2019). Rani and co-worker reported the highest specific capacity using fluorinated graphite based cathode (Rani et al., 2013). The improved capacity obtained is attributable to increased electrophilicity of the fluorinated graphite. Improved stability was reported with  $\text{V}_2\text{O}_5/\text{C}$  reported when  $\text{AlCl}_3$ -dipropylsulfone-toluene (1:10:5 in mole ratio) was used as electrolyte (Chiku et al., 2015). The improvement may be attributed to reduction of corrosive impact of  $[\text{AlCl}_4]^-$  on the  $\text{V}_2\text{O}_5/\text{C}$  by toluene. With regards  $[\text{AlCl}_4]^-$  intercalation, protonated polyaniline can electrostatically intercalate  $[\text{AlCl}_4]^-$ , or least improved  $[\text{AlCl}_4]^-$  intercalation can be achieved using polyaniline-graphite composite than mere graphite. It is surprising that there are scanty reports in this direction. The only study in this direction examined Polyaniline/ $\text{AlCl}_3$ -1-ethyl-3-methylimidazolium chloride/Polyaniline cell. A charge/discharge efficiency 99% obtained showed that polyaniline is compatible with electrolyte (Koura, 1993).

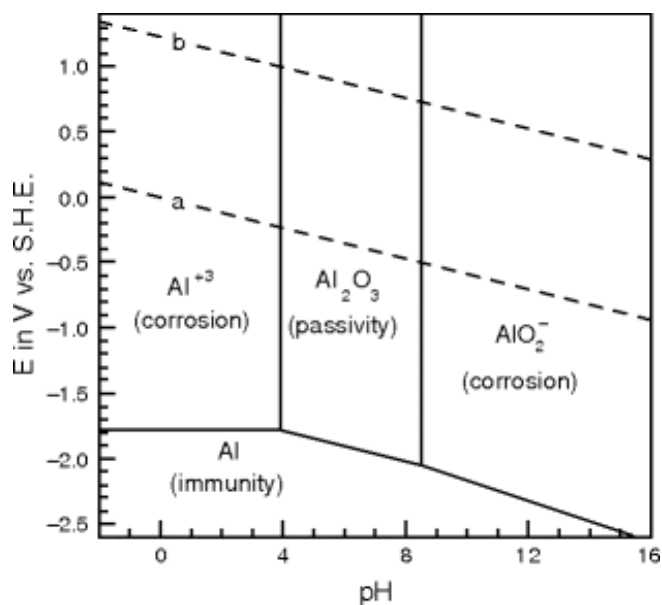
Taking a cue from lithium battery, sulphur is the most promising cathode for aluminium battery in

**Table 14:** Proposed cell of Aluminium-sulphur battery in  $\text{AlCl}_3$ -1-ethyl-3-methylimidazolium chloride electrolyte (Yang et al., 2018)

|                            |   |
|----------------------------|---|
| Anodic half reaction       | $2\text{Al} + 8\text{AlCl}_4^- + 2n(\text{Urea}) \rightarrow 2[\text{AlCl}_2(\text{Urea})_n]^+ + 4\text{Al}_2\text{Cl}_7^- + 6e^-$  |
| Cathodic reactions         | $\text{Al}_2\text{Cl}_6\text{Br} \rightarrow \text{AlCl}_3 + \text{AlCl}_3\text{Br} \rightarrow \text{AlCl}_3\text{Br} + \frac{3}{4}\text{AlCl}_4^- + \frac{1}{4}\text{Al}^{3+}$<br>$\text{Al}_2\text{Cl}_7^- \rightarrow \text{AlCl}_3 + \text{AlCl}_4^- \rightarrow \frac{7}{4}\text{AlCl}_4^- + \frac{1}{4}\text{Al}^{3+}$<br>$2\text{Al}^{3+} + 3\text{S} + 6e^- \rightarrow \text{Al}_2\text{S}_3$ |
| Net Cathodic half reaction | $8\text{Al}_2\text{Cl}_7^- + 3\text{S} + 6e^- \rightarrow \text{Al}_2\text{S}_3 + 14\text{AlCl}_4^-$  |
| Overall reaction           | $2\text{Al} + 4\text{Al}_2\text{Cl}_7^- + 3\text{S} + 2n(\text{Urea}) \rightarrow \text{Al}_2\text{S}_3 + 2[\text{AlCl}_2(\text{Urea})_n]^+ + 6\text{AlCl}_4^-$   |



a. Pourbaire diagram of zinc (McCafterty, 2010)



b. Pourbaire diagram of aluminium (Zhu and Hihara, 2010)

**Figure 15:** Equilibrium phases of zinc and aluminium in aqueous media

terms of capacity and cost. In recent times, attention is gradually shifting towards studies on sulphur cathode for  $\text{AlCl}_3$ -halide salt melts electrolytes Al-ion batteries. Aluminium battery can benefit from sulphur cathode preparation techniques already established for lithium-sulphur battery. Polyaniline-sulphur-graphite composite will make a practical combination. It has been found that the cathodic reaction of aluminium-sulphur battery with  $\text{AlCl}_3$ -1-ethyl-3-methylimidazolium chloride electrolyte is a multi-step CE (chemical-electrochemical) process. The chemical step which involves formation aluminium cation is rate limiting due slow rate of dissociation of

heptachlorodialuminate anion ( $\text{Al}_2\text{Cl}_7^-$ ). However, rate of dissociation of heptachlorodialuminate anion can be catalysed by bromide ion ( $\text{Br}^-$ ). This was attributed to weaker bridge bond in  $\text{Al}_2\text{Cl}_6\text{Br}$  compared to  $\text{Al}_2\text{Cl}_7^-$  (Yang et al., 2018). The proposed cell reaction is shown in Table 14.

#### 4.3.3. Water-in-salt electrolyte

After several decades of exploration of  $\text{AlCl}_3$ -halide salts melts chemistry for aluminium ion battery, it was realised that electro-deposition of aluminium in aqueous is possible. It was realised that oxophilic nature

of aluminium is not a hindrance to electroplating and stripping of aluminium in aqueous system. Perhaps inspired by similarity of their Pourbaix diagrams (Figure 15), aqueous aluminium battery should be possible by building on Zn-MnO<sub>2</sub> battery templates. There are two main long standing obstacles of aqueous aluminium battery: first, the potential of aluminium electroplating/stripping is more negative than that of zinc resulting in extensive hydrogen evolution. Although, the pursuit of non-aqueous aluminium battery avoids hydrogen evolution problem, but new challenges surfaced. In the case of zinc ion battery, hydrogen evolution problem was kinetically prevented by use concentrated zinc salt solution as electrolyte. Albeit with modification that satisfies peculiar chemistry of aluminium ion (Al<sup>3+</sup>), the strategy can be adopted for aqueous aluminium battery.

The second concern obstacle against aqueous aluminium ion battery is the long held view that reversible intercalation/de-intercalation of highly charged Al<sup>3+</sup> ions into/out of common layered cathode materials will be very difficult. Because of its high ionic charge density (Al<sup>3+</sup> is smaller than Zn<sup>2+</sup>), its large hydration/solvation sphere will be a drag against efficient ionic diffusion and intercalation/de-intercalation into/out of a prospective cathode material (Latha & Vatsala Rani, 2020). Use of aluminium salts with bulky hydrophobic anion can help minimise hydration atmosphere of Al<sup>3+</sup> ions. This had been exploited in organic synthesis to take advantage of catalytic property of Lewis acidity of Al<sup>3+</sup> in aqueous media (Antoniotti et al., 2010). Use of bulky hydrophobic anion now comes in handy towards realisation of aqueous aluminium battery. Aluminium salts of bis(trifluoromethanesulfonyl)imide Al(TFSI)<sub>3</sub> and trifluoromethanesulfonate Al(TfO)<sub>3</sub> have enabled functional aluminium aqueous batteries. Also, the hydration/solvation concern can be minimised by use of concentrated electrolyte solution otherwise known as ‘*Water-in-Salt Electrolyte*’ (Suo et al., 2015). Functional aqueous aluminium batteries had been achieved using AlCl<sub>3</sub> water-in-salt electrolyte (Hu et al., 2020). Moreover, since aluminium has similar chemistry as zinc, Al<sup>3+</sup> ions do not necessarily have to undergo intercalation/de-intercalation, provided the cathode reaction involves proton uptake, like in the case of Zn-MnO<sub>2</sub> battery (J. Wang et al., 2019), the resulting pH increase of the electrolyte will precipitate Al<sup>3+</sup> as Al(OH)<sub>3</sub> (Table 15).

Dissolution of the Al(OH)<sub>3</sub> will take place during charging. Water-in-salt electrolyte also encourages pillaring of the layered framework structure cathode materials by hydrated cations. For example, high cycle life spans obtained in some reported Zn-ion batteries had been attributed to formation and stabilisation layered structures of MnO<sub>2</sub>, V<sub>2</sub>O<sub>5</sub> by hydrated Zn<sup>2+</sup> and Ca<sup>2+</sup> ions

(Liu et al., 2019; W. Zhang et al., 2019). Similar pillaring effect had been observed in Al-MnO<sub>2</sub> aqueous battery (Huang et al., 2018; Zhao et al., 2018) although yet to be reported the same may be expected for Al-V<sub>2</sub>O<sub>5</sub> aqueous battery.

**Table 15:** Cell reaction for Al-MnO<sub>2</sub> battery water-in-salt electrolyte

| Electrode             | Electrode & cell reaction   |
|-----------------------|---|
| Anode half reaction   | $2\text{Al}_{(s)} \rightarrow 2\text{Al}_{(aq)}^{3+} + 6e^{-}$  |
| Cathode half reaction | $3\text{H}_2\text{O}_{(l)} \rightleftharpoons 6\text{H}_{(aq)}^{+} + 6\text{OH}_{(aq)}^{-}$ $6\text{MnO}_{2(s)} + 6\text{H}_{(aq)}^{+} + 2e^{-} \rightarrow 6\text{MnOOH}_{(s)}$ $2\text{Al}_{(aq)}^{3+} + 6\text{OH}_{(aq)}^{-} \rightarrow 2\text{Al(OH)}_{3(s)}$ |
| Overall reaction      | $2\text{Al}_{(s)} + 6\text{MnO}_{2(s)} + 3\text{H}_2\text{O}_{(l)} \rightleftharpoons$ $2\text{Al(OH)}_{3(s)} + 6\text{MnOOH}_{(s)}$  |

From Al<sub>2</sub>O<sub>3</sub>-cryolite melt through AlCl<sub>3</sub>-halide salt melts to water-in-salt electrolyte, electroplating/stripping of aluminium has move from irreversible high energy intensive to a green reversible process. The recent possibility has set aluminium as promising anode material for aqueous and non-aqueous batteries. Research and developments in aluminium battery is poised to proceed at a faster rate because of the benefits of established methods and techniques from zinc and lithium batteries. Aqueous aluminium battery will surpass zinc battery in specific capacity and thus compete in zinc in some portable applications. Albeit low specific capacity, non-aqueous aluminium-sulphur battery will be a lower cost alternative to lithium-sulphur battery, and a promising new entry to the battery market.

#### 4.4. Liquid metal battery

In another inspiration from the aluminium electrometallurgy, motivated by its capacity for continuous operation and consuming huge amount of electricity in the process. The advocates of liquid metal battery reasoned that the process could be modified to operate reversibly; it will engender low cost grid level electricity storage. As the name implies, liquid metal battery is an all-liquid electrochemical cell. Although the ideal of exploiting all-liquid electrochemical cell for electricity storage is not new, but recent contribution by Sadoway and co-workers to the area has bring about renaissance of interest in liquid metal battery (Kim, Boysen, Newhouse, et al., 2013). A three-liquid-layer Hoopes cell for the electrolytic production of high-purity aluminium is the first all-liquid electrochemical cell. It consisted of a high-density Cu–Al alloy as bottom

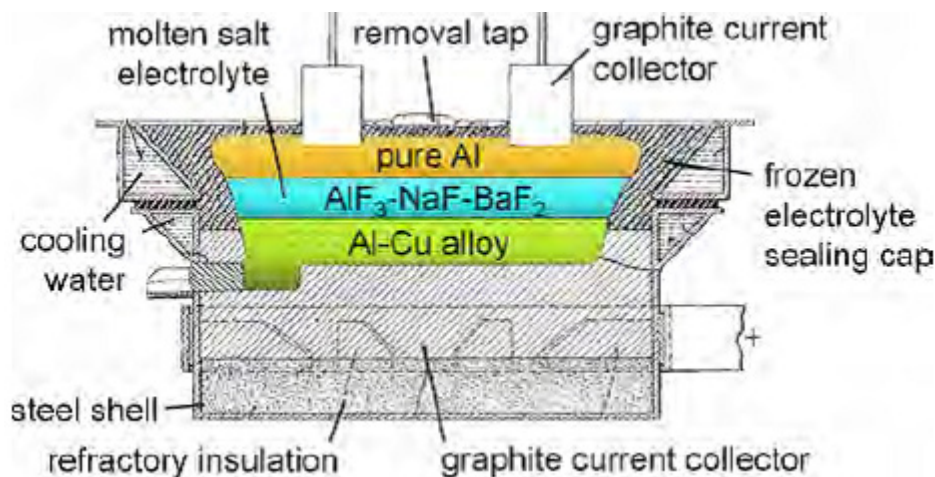


**Figure 16:** Diagram of a Hoopes cell showing a three-liquid-layer electrolytic cell for the purification of aluminium (Kim, Boysen, Newhouse, et al., 2013)

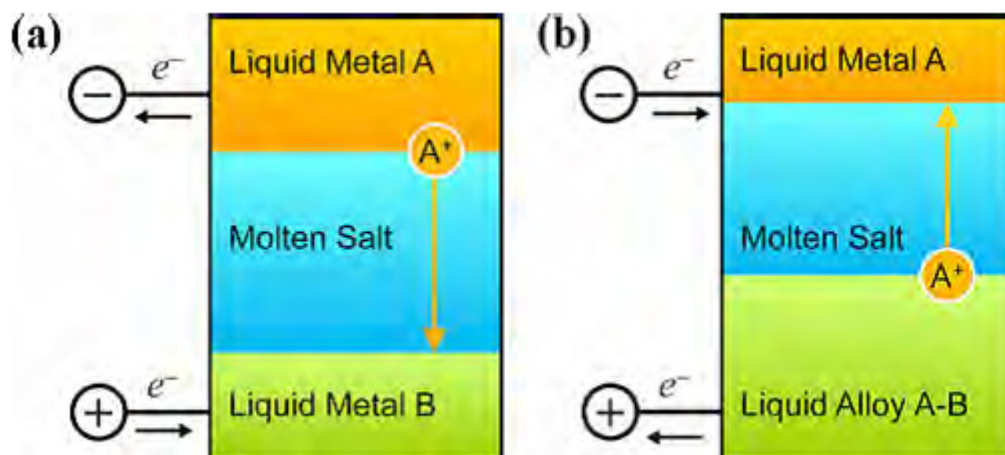


**Figure 17:** Schematic diagram of a liquid metal battery upon (a) discharging (b) charging (Kim, Boysen, Newhouse, et al., 2013)

anode, and a low-density, high-purity liquid aluminium as top cathode, the two electrodes separated by a molten salt electrolyte Figure 16.

Liquid metal battery shares the same configuration as the Hoopes cell, it consists a molten salt electrolyte sandwiched by two liquid metal electrodes. The electrodes and the electrolyte self-segregate into three layers on the basis of density and immiscibility. Schematic diagram of operation liquid metal battery is presented in Figure 17. During discharging the anode, metal undergoes oxidation-releasing electron which passes through the conductor. The resulting cation migrates through the electrolyte to the cathode. At the cathode, the cation accepts electron becomes reduced and forms alloy with cathode. The whole process is reversed during charging. The driving force for the discharging

is the positive difference of reduction potential of the electrode and enthalpy of alloy formation.

Metal selection as electrode for liquid metal battery is based on difference in electrode potential of the anode candidate and cathode candidate. Categorisation for this purpose is depicted in Figure 18. The anode candidates have low electronegativity while the cathode candidates have high electronegativity. A liquid metal battery may be obtained by pairing metals from either side of the divide in Figure 18. For instance, magnesium-antimony pair was reported by Bradwell et al. (2012). They used  $\text{MgCl}_2\text{-KCl-NaCl}$  mix as electrolyte, magnesium as anode and antimony as cathode. The cell was denoted  $\text{Mg}||\text{Sb}$  and operates at  $700^\circ\text{C}$ , schematic of it operation is shown in Figure 19. The cell performance was adjudged promising, its high operating temperature was



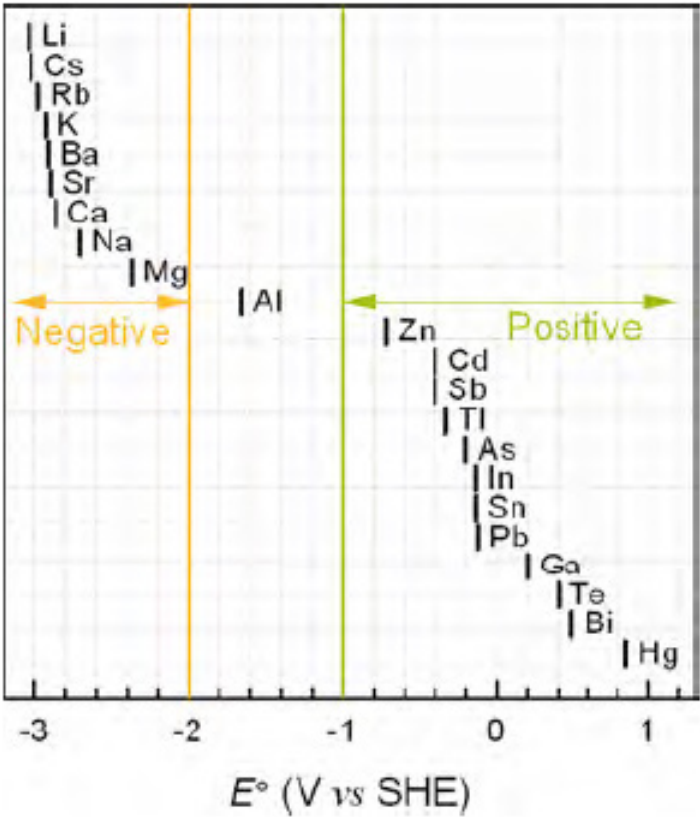


**Figure 18:** Electrode candidates for liquid metal battery, Anodes negative (orange) and Cathodes (green) (Kim, Boysen, Newhouse, et al., 2013)

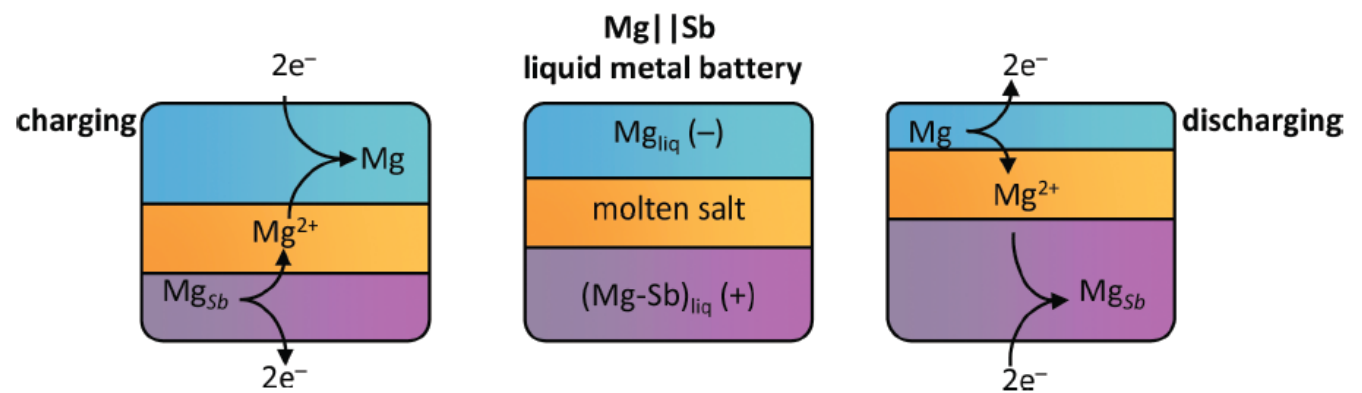


**Figure 19:** Schematic of Mg||Sb liquid metal battery comprising three liquid layers that operates at 700 °C (Bradwell et al., 2012)

**Table 16:** Reported liquid metal battery and their operating temperatures

| Electrode pair                      | Operating temperature (°C) | References                         |
|-------------------------------------|----------------------------|------------------------------------|
| Mg  MgCl <sub>2</sub> –KCl–NaCl  Sb | 700                        | (Bradwell et al., 2012)            |
| Li LiF–LiCl–LiBr Sb–Sn              | 500                        | (H. Li et al., 2016)               |
| Li LiF–LiCl–LiBr Sb–Pb              | 450                        | (K. Wang et al., 2014)             |
| Ca LiCl–NaCl–CaCl <sub>2</sub>   Bi | 500-700                    | (Kim, Boysen, Ouchi, et al., 2013) |
| Li LiCl–LiBr Bi                     | 550                        | (Ning et al., 2015)                |

a disadvantage, hence a lower operating temperatures couples was desired. Other explored electrode couples and their operating temperature is shown in Table 16. So far, lowest reported operating temperature is 450 °C which still is consider high and a disadvantage for suitability for portable applications. The corrosive nature of the active cell components, high tendency for self-discharge and short-circuiting due to sensitivity to motion during operation, may discourage widespread adoption. Nonetheless, simple assembly, low materials cost, and long cycle life span are appeals of liquid metal battery for grid-scale storage applications.

## 5. Conclusion

Global warming and climate change are main drivers of the need to increase the proportion of renewable electricity in the global energy mix. With sustained investments in solar and wind electricity, capacities of renewable energy sources will stand shoulder high with fossil fuels consumption. However, the full benefits of solar and wind electricity cannot be realised without grid storage capacity. Hence, battery is an essential complement in order to realise the full benefit of solar and wind electricity. Since battery is a devise for chemical-electrical energy inter-conversion, the usefulness of a battery depends on its chemistry. Therefore, in this contribution, we examined the chemistries of existing commercial and emerging batteries focusing on lead-acid, zinc-alkaline, lithium ion, aluminium and liquid metal batteries. Despite its low specific capacity, simple assembly and rugged cell operation had kept lead-acid battery not only at the top of battery market but also a leading contender for grid-scale applications. Zinc-alkaline suffers from poor cycle life span due to fragile cell assembly and low cell voltage due to constraints of aqueous electrolyte and thus dwindling market share. Emerging zinc batteries using neutral electrolyte and solid electrolyte should produce resurgent zinc batteries that will reclaim lost market share and command new ones including grid-scale storage applications. The success of rocking chair chemistry has enabled lithium ion battery to calf a niche in the mobile and portable electronics applications. It is currently expanding into the electric vehicle applications and beyond. But it is yet to be a good contender in the grid-scale application because of its high cost. Aluminium had emerged from obscurity of Hall-Héroult electrolysis cell to a promising battery material. It has ability to combine some of the strengths of zinc ion and lithium ion batteries. Although there is yet a commercial aluminium battery, it is predicted that aluminium battery will enter the market

in the nearest foreseeable future. In addition, it may be a strong contender with lead-acid for grid-scale applications. Liquid metal battery is strictly designed for grid-scale storage applications. It has advantage of simple assembly, low materials cost, and long cycle life span. However, high operating temperature and corrosion problem are its Achilles' heel.

## References

- Angell, M., Pan, C. J., Rong, Y., Yuan, C., Lin, M. C., Hwang, B. J., & Dai, H. (2017). High Coulombic efficiency aluminum-ion battery using an  $\text{AlCl}_3$ -urea ionic liquid analog electrolyte. *PNAS*, 114(5), 834–839.
- Antoniotti, S., Dalla, V., & Duñach, E. (2010). Metal triflimidates: Better than metal triflates as catalysts in organic synthesis-the effect of a highly delocalized counteranion. *Angewandte Chemie - International Edition*, 49(43), 7860–7888.
- Ayres, R. U., Van den Bergh, J. C. J. M., Lindenberger, D., & Warr, B. (2013). The underestimated contribution of energy to economic growth. *Structural Change and Economic Dynamics*, 27, 79–88.
- Bahceci, S., & Esat, B. (2013). A polyacetylene derivative with pendant TEMPO group as cathode material for rechargeable batteries. *Journal of Power Sources*, 242, 33–40.
- Bian, Y., Li, Y., Yu, Z., Chen, H., Du, K., Qiu, C., Zhang, G., Lv, Z., & Lin, M. C. (2018). Using an  $\text{AlCl}_3$ /Urea ionic liquid analog electrolyte for improving the lifetime of aluminum-sulfur batteries. *ChemElectroChem*, 5(23), 3607–3611.
- Böttcher, R., Valitova, A., Ispas, A., & Bund, A. (2019). Electrodeposition of aluminium from ionic liquids on high strength steel. *Transactions of the Institute of Metal Finishing*, 97(2), 82–88.
- Bradwell, D. J., Kim, H., Sirk, A. H. C., & Sadoway, D. R. (2012). Magnesium-antimony liquid metal battery for stationary energy storage. *Journal of the American Chemical Society*, 134(4), 1895–1897.
- Breeze, P. (2017). The carbon cycle and atmospheric warming. *Electricity generation and the environment* (pp. 13–21). Academic Press.
- Cai, P., Wang, G., Chen, K., & Wen, Z. (2019). Reversible Zn-quinone battery with harvesting electrochemical neutralization energy. *Journal of Power Sources*, 428, 37–43.
- Capuano, G. A. (1991). The electrodeposition of aluminum and aluminum alloys from alkylbenzene-hbr electrolytes. *Journal of The Electrochemical Society*, 138(2), 484–490.
- Chang, J., Shang, J., Sun, Y., Ono, L. K., Wang, D., Ma, Z., Huang, Q., Chen, D., Liu, G., Cui, Y., Qi, Y., & Zheng, Z. (2018). Flexible and stable high-energy lithium-sulfur

- full batteries with only 100% oversized lithium. *Nature Communications*, 9(1), 1–11.
- Chen, H., Cong, T. N., Yang, W., Tan, C., Li, Y., & Ding, Y. (2009). Progress in electrical energy storage system: A critical review. *Progress in Natural Science* 19(3), 291–312.
- Chiku, M., Takeda, H., Matsumura, S., Higuchi, E., & Inoue, H. (2015). Amorphous vanadium oxide/carbon composite positive electrode for rechargeable aluminum battery. *ACS Applied Materials and Interfaces*, 7(44), 24385–24389.
- Delahay, P., Pourbaix, M., & Van Rysselberghe, P. (1951). Potential-pH diagram of zinc and its applications to the study of zinc corrosion. *Journal of The Electrochemical Society*, 98(3), 101.
- Fang, Y., Yoshii, K., Jiang, X., Sun, X. G., Tsuda, T., Mehio, N., & Dai, S. (2015). An  $\text{AlCl}_3$  based ionic liquid with a neutral substituted pyridine ligand for electrochemical deposition of aluminum. *Electrochimica Acta*, 160, 82–88.
- Frk, M., Maca, J., & Rozsivalova, Z. (2013). Study of dynamic viscosity and density of aprotic solvents for lithium – ion batteries. *RE&PQJ*, 1(11), 778–782.
- Galashev, A. Y. and Ivanichkina, K. A. (2018). Computer Study of atomic mechanisms of intercalation/deintercalation of Li Ions in a silicene anode on an Ag (111) substrate. *Journal of The Electrochemical Society*, 165(9), A1788–A1796.
- Gauthier, M., Carney, T. J., Grimaud, A., Giordano, L., Pour, N., Chang, H. H., Fenning, D. P., Lux, S. F., Paschos, O., Bauer, C., Maglia, F., Lupart, S., Lamp, P., & Shao-Horn, Y. (2015). Electrode-Electrolyte Interface in Li-Ion Batteries: Current Understanding and New Insights. *Journal of Physical Chemistry Letters*, 6(22), 4653–4672.
- Gür, T. M. (2018). Review of electrical energy storage technologies, materials and systems: Challenges and prospects for large-scale grid storage. *Energy and Environmental Science*, 11(10), 2696–2767.
- Hasanuzzaman, M., Zubir, U. S., Ilham, N. I., & Seng Che, H. (2016). Global electricity demand, generation, grid system, and renewable energy policies: A review. *WIREs Energy and Environment*, 6(3), e222.
- Hong, X., Mei, J., Wen, L., Tong, Y., Vasileff, A. J., Wang, L., Liang, J., Sun, Z., & Dou, S. X. (2019). Nonlithium metal–sulfur batteries: steps toward a leap. *Advanced Materials*, 31, 1802822, 1–30.
- Hu, Z., Guo, Y., Jin, H., Ji, H., & Wan, L.-J. (2020). A rechargeable aqueous aluminum–sulfur battery through acid activation in water-in-salt electrolyte. *Chem. Commun.*, 56, 2023–2026.
- Huang, H., Strømme, M., Gogoll, A., & Sjö, M. (2013). Polymer – pendant interactions in poly (pyrrol-3-ylhydroquinone): A solution for the use of conducting polymers at stable conditions. *The Journal of Physical Chemistry C*, 117, 45, 23558–23567.
- Huang, J., Wang, Z., Hou, M., Dong, X., Liu, Y., Wang, Y., & Xia, Y. (2018). Polyaniline-intercalated manganese dioxide nanolayers as a high-performance cathode material for an aqueous zinc-ion battery. *Nature Communications*, 9(1), 1–8.
- Huang, S., Sun, J., Yan, J., Liu, J., Wang, W., Qin, Q., Mao, W., Xu, W., Wu, Y., & Wang, J. (2018). Enhanced high-temperature cyclic stability of al-doped manganese dioxide and morphology evolution study through in situ nmr under high magnetic field. *ACS Applied Materials and Interfaces*, 10(11), 9398–9406.
- Jafarian, M., Mahjani, M. G., Gobal, F., & Danaee, I. (2006). Electrodeposition of aluminum from molten  $\text{AlCl}_3$ -NaCl-KCl mixture. *Journal of Applied Electrochemistry*, 36(10), 1169–1173.
- Julien, C. M., & Mauger, A. (2017). Nanostructured  $\text{MnO}_2$  as electrode materials for energy storage. *Nanomaterials*, 7(11), 396. doi:10.3390/nano7110396.
- Keith, J. R., & Ganesan, V. (2020). Ion transport mechanisms in salt-doped polymerized zwitterionic electrolytes. *Journal of Polymer Science*, 58, 578–588.
- Kim, H., Boysen, D. A., Newhouse, J. M., Spatocco, B. L., Chung, B., Burke, P. J., Bradwell, D. J., Jiang, K., Tomaszowska, A. A., Wang, K., Wei, W., Ortiz, L. A., Barriga, S. A., Poizeau, S. M., & Sadoway, D. R. (2013). Liquid metal batteries: Past, present, and future. *Chemical Reviews*, 113(3), 2075–2099.
- Kim, H., Boysen, D. A., Ouchi, T., & Sadoway, D. R. (2013). Calcium-bismuth electrodes for large-scale energy storage (liquid metal batteries). *Journal of Power Sources*, 241, 239–248.
- Kirchman, D. L. (2008). Introduction and overview. *Microbial ecology of the oceans* (2<sup>nd</sup> ed., pp. 1–26). John Wiley & Sons.
- Kitada, A., Nakamura, K., Fukami, K., & Murase, K. (2016). Electrochemically active species in aluminum electrodeposition baths of  $\text{AlCl}_3$ /glyme solutions. *Electrochimica Acta*, 211, 561–567.
- Koura, N. (1993). Polyaniline secondary cells with ambient temperature molten salt electrolytes. *Journal of The Electrochemical Society*, 140(3), 602–605.
- Kvande, H. (2010). Production of primary aluminium. *Fundamentals of Aluminium Metallurgy: Production, Processing and Applications*, 49–69.
- Lai, P. K. (1989). Electrodeposition of aluminium and its dissolution in room temperature molten salts [Ph.D thesis]. School of Chemical Engineering and Industrial Chemistry, University of New South Wales, Australia.
- Latake, P. T., Pawar, P., & Ranveer, A. C. (2015). The greenhouse effect and its impacts on environment.

- International Journal of Innovative Research and Creative Technology Wwww.Ijirct.Org*, 1(3), 333-337.
- Latha, M., & Vatsala Rani, J. (2020). WS<sub>2</sub>/Graphene Composite as Cathode for Rechargeable Aluminum-Dual Ion Battery. *Journal of The Electrochemical Society*, 167(7), 070501.
- Leisegang, T., Meutzner, F., Zschornak, M., Münchgesang, W., Schmid, R., Nestler, T., Eremin, R. A., Kabanov, A. A., Blatov, V. A., & Meyer, D. C. (2019). The aluminum-ion battery: A sustainable and seminal concept? *Frontiers in Chemistry*, 7(APR), 1–21.
- Li, H., Wang, K., Cheng, S., & Jiang, K. (2016). High performance liquid metal battery with environmentally friendly antimony-tin positive electrode. *ACS Applied Materials and Interfaces*, 8(20), 12830–12835.
- Li, M., Gao, B., Liu, C., Chen, W., Wang, Z., Shi, Z., & Hu, X. (2017). AlCl<sub>3</sub>/amide ionic liquids for electrodeposition of aluminum. *Journal of Solid State Electrochemistry*, 21(2), 469–476.
- Li, S., Zhang, G., Jing, G., & Kan, J. (2008). Aqueous zinc-polyaniline secondary battery. *Synthetic Metals*, 158(6), 242–245.
- Li, W., Zheng, G., Yang, Y., Seh, Z. W., Liu, N., & Cui, Y. (2013). High-performance hollow sulfur nanostructured battery cathode through a scalable, room temperature, one-step, bottom-up approach. *PNAS*, 110(18), 7148–7153.
- Liu, X., Zhang, H., Geiger, D., Han, J., Varzi, A., Kaiser, U., Moretti, A., & Passerini, S. (2019). Calcium vanadate sub-microfibers as highly reversible host cathode material for aqueous zinc-ion batteries. *Chem. Commun.*, 55(16), 2265–2268.
- Liu, Z., Huang, Y., Huang, Y., Yang, Q., Li, X., Huang, Z., Zhi, C. (2020). Voltage issue of aqueous rechargeable metal-ion batteries. *Chemical Society Review*, 49, 180–232.
- Lu, F., Gao, X., Wu, A., Sun, N., Shi, L., & Zheng, L. (2017). Lithium-containing zwitterionic poly(ionic liquid)s as polymer electrolytes for lithium-ion batteries. *Journal of Physical Chemistry C*, 121(33), 17756–17763.
- Lumen, Chemistry for Non-Majors, Electrochemistry. 2020. <https://courses.lumenlearning.com/cheminter/chapter/electrochemistry/>
- Mainar, A. R., Colmenares, L. C., Leonet, O., Alcaide, F., Irui, J. J., Weinberger, S., Hacker, V., Irui, E., Urdanpilleta, I., & Blazquez, J. A. (2016). Manganese oxide catalysts for secondary zinc air batteries: from electrocatalytic activity to bifunctional air electrode performance. *Electrochimica Acta* 217, 80–91.
- Magnuson, M., Guo, J.-H., Butorin, S. M., Agui, A., Sâthe, C., Nordgren, J., Monkman, A. P. (1999) The electronic structure of polyaniline and doped phases studied by soft X-ray absorption and emission spectroscopies, *Journal of Chemical Physics*, 111, 4756, 1-8.
- McCafferty, E. (2010). Introduction to corrosion science. *Introduction to corrosion science*. Springer.
- Minakshi, M. (2009). Improved performance of Bi<sub>2</sub>O<sub>3</sub>-doped MnO<sub>2</sub> cathode on rechargeability in LiOH aqueous cell. *Journal of Solid State Electrochemistry*, 13(8), 1209–1214.
- Munaoka, T., Yan, X., Lopez, J., To, J. W. F., Park, J., Tok, J. B. H., Cui, Y., & Bao, Z. (2018). Ionically conductive self-healing binder for low cost si microparticles anodes in Li-Ion batteries. *Advanced Energy Materials*, 8(14), 1–11.
- Ning, X., Phadke, S., Chung, B., Yin, H., Burke, P., & Sadoway, D. R. (2015). Self-healing Li-Bi liquid metal battery for grid-scale energy storage. *Journal of Power Sources*, 275, 370–376.
- Nitta, N., Wu, F., Lee, J. T., & Yushin, G. (2015). Li-ion battery materials: Present and future. *Materials Today*, 18(5), 252–264.
- Olugbenga, F. P. (2009). Energy exploitation, utilization, and its environmental effects - the choice to make and the decision to take. *Toxicological and Environmental Chemistry*, 91(5), 1015–1019.
- Pan, K., Shi, G., Li, A., Li, H., Zhao, R., Wang, F., Zhang, W. & Chen, Q., Chen, H., Xiong, Z., & Finlow, D. (2012). The performance of a silica-based mixed gel electrolyte in lead acid batteries. *Journal of Power Sources*, 209, 262–268 <https://doi.org/10.1016/j.jpowsour.2012.02.101>
- Pargoletti, E., Cappelletti, G., Minguzzi, A., Rondinini, S., Leoni, M., Marelli, M., & Vertova, A. (2016). High-performance of bare and Ti-doped  $\alpha$ -MnO<sub>2</sub> nanoparticles in catalyzing the oxygen reduction reaction. *Journal of Power Sources*, 325, 116–128.
- Patel, S. (2019, November 14). IEA world energy outlook: Solar capacity surges past coal and gas by 2040. <https://www.powermag.com/iea-world-energy-outlook-solar-capacity-surges-past-coal-and-gas-by-2040/>
- Peled, E. (1979). The electrochemical behavior of alkali and alkaline earth metals in nonaqueous battery systems—the solid electrolyte interphase model. *Journal of The Electrochemical Society*, 126(12), 2047.
- Popov, B. N. (2015). Thermodynamics in the Electrochemical reactions of corrosion, corrosion engineering (pp. 29-91). Elsevier.
- Prengaman, R. D. (1991). Improved grid alloys for deep-cycling lead calcium batteries. *Journal of Power Sources*, 33(1-4), 13-20.
- Quaino, P., Juarez, F., Santos, E., & Schmickler, W. (2014). Volcano plots in hydrogen electrocatalysis-uses and abuses. *Beilstein Journal of Nanotechnology*, 5(1), 846–854.
- Rahmanifar, M. S., Mousavi, M. F., & Shamsipur, M. (2002). Effect of self-doped polyaniline on performance of secondary Zn – polyaniline battery. *Journal of Power Sources*, 110(1), 229–232.



- Rani, J. V., Kanakaiah, V., Dadmal, T., Rao, M. S., & Bhavanarushi, S. (2013). Fluorinated natural graphite cathode for rechargeable ionic liquid based aluminum-ion battery. *Journal of The Electrochemical Society*, 160(10), A1781–A1784.
- Salameh, Z. (2014). Factors promoting renewable energy applications. *Renewable Energy System Design* (pp. 1–32). Academic Press.
- Seh, Z. W., Li, W., Cha, J. J., Zheng, G., Yang, Y., McDowell, M. T., Hsu, P. C., & Cui, Y. (2013). Sulphur-TiO<sub>2</sub> yolk-shell nanoarchitecture with internal void space for long-cycle lithium-sulphur batteries. *Nature Communications*, 4, 1331. doi:10.1038/ncoms2327.
- Shaibani, M., Mirshekarloo, M. S., Singh, R., Easton, C. D., Dilusha Cooray, M. C., Eshraghi, N., Abendroth, T., Dörfler, S., Althues, H., Kaskel, S., Hollenkamp, A. F., Hill, M. R., & Majumder, M. (2020). Expansion-tolerant architectures for stable cycling of ultrahigh-loading sulfur cathodes in lithium-sulfur batteries. *Science Advances*, 6, eaay2757.
- Shi, H.-Y., Ye, Y.-J., Liu, K., Song, Y., Sun, X. (2018). A Long cycle-life self-doped polyaniline cathode for rechargeable aqueous zinc batteries. *Angewandte Chemie International Edition*, 57(50), 16359–16363.
- Shi, J., Zhang, J., & Guo, J. (2019). Avoiding pitfalls in rechargeable aluminum batteries research. *ACS Energy Letters*, 4(9), 2124–2129.
- Shin, J., Seo, J. K., Yaylian, R., Huang, A., & Meng, Y. S. (2019). A review on mechanistic understanding of MnO<sub>2</sub> in aqueous electrolyte for electrical energy storage systems. *International Materials Reviews*. doi:10.1080/09506608.2019.1653520.
- Sun, M., Lin, T., Cheng, G., Ye, F., & Yu, L. (2014a). Hydrothermal synthesis of boron-doped MnO<sub>2</sub> and its decolorization performance. *Journal of Nanomaterials*, 2014, 1–6. doi:10.1155/2014/175924.
- Sun, Y., Wang, S., Dai, Y., & Lei, X. (2016). Electrochemical characterization of nano V, Ti doped MnO<sub>2</sub> in primary lithium manganese dioxide batteries with high rate. *Functional Materials Letters*, 9(1). doi:10.1142/S1793604716500053.
- Suo, L., Borodin, O., Gao, T., Olguin, M., Ho, J., Fan, X., Luo, C., Wang, C., & Xu, K. (2015). “Water-in-salt” electrolyte enables high-voltage aqueous lithium-ion chemistries. *Science*, 350(6263), 938–943.
- Tang, B., Shan, L., Liang, S., & Zhou, J. (2019). Issues and opportunities facing aqueous zinc-ion batteries. *Energy and Environmental Science*, 12(11), 3288–3304.
- Technopark, Y. (2017). A novel gel electrolyte for valve-regulated lead acid battery. *Anadolu University Journal of Science and Technology A- Applied Sciences and Engineering*, 18(1), 146 - 160.
- The Royal Swedish Academy of Sciences. (2019). Scientific background on the nobel prize in chemistry 2019 lithium-ion batteries. *The Royal Swedish Academy of Science*, 50005, 0–13.
- Tiyapiboonchaiya, C., Pringle, J. M., Sun, J., Byrne, N., Howlett, P. C., MacFarlane, D. R., & Forsyth, M. (2004). The zwitterion effect in high-conductivity polyelectrolyte materials. *Nature Materials*, 3(1), 29–32.
- Trasatti, S. (1984). Electrocatalysis in the anodic evolution of oxygen and chlorine. *Electrochimica Acta*, 29(11), 1503–1512.
- Tu, X., Zhang, J., Zhang, M., Cai, Y., Lang, H., Tian, G., & Wang, Y. (2017). Electrodeposition of aluminium foils on carbon electrodes in low temperature ionic liquid. *RSC Advances*, 7(24), 14790–14796.
- U. S. Energy Information Administration (2011, September 28) Renewable energy shows strongest growth in global electric generating capacity. <https://www.eia.gov/todayinenergy/detail.php?id=3270>
- Venugopalan, S. (1993). Influence of phosphoric acid on the electrochemistry of lead electrodes in sulfuric acid electrolyte containing antimony, *Journal of Power Sources*, 46, 1–15.
- Venugopalan, S., Division, B., & Group, P. S. (1994). Kinetics of hydrogen-evolution reaction on lead and lead-alloy electrodes in sulfuric acid electrolyte with phosphoric acid and antimony additives. *Journal of Power Sources*, 48, 371–384.
- Wang, C., Wu, H., Chen, Z., McDowell, M. T., Cui, Y., & Bao, Z. (2013). Self-healing chemistry enables the stable operation of silicon microparticle anodes for high-energy lithium-ion batteries. *Nature Chemistry*, 5(12), 1042–1048.
- Wang, D., Wang, L., Liang, G., Li, H., Liu, Z., Tang, Z., Liang, J., & Zhi, C. (2019). A superior δ-MnO<sub>2</sub> cathode and a self-healing Zn-δ-MnO<sub>2</sub> Battery. *ACS Nano*, 13(9), 10643–10652.
- Wang, J., Wang, J. G., Liu, H., Wei, C., & Kang, F. (2019). Zinc ion stabilized MnO<sub>2</sub> nanospheres for high capacity and long lifespan aqueous zinc-ion batteries. *Journal of Materials Chemistry A*, 7(22), 13727–13735.
- Wang, K., Jiang, K., Chung, B., Ouchi, T., Burke, P. J., Boysen, D. A., Bradwell, D. J., Kim, H., Muecke, U., & Sadoway, D. R. (2014). Lithium-antimony-lead liquid metal battery for grid-level energy storage. *Nature*, 514(7522), 348–350.
- Xu, K. (2004). Nonaqueous liquid electrolytes for lithium-based rechargeable batteries. *Chemical Reviews*, 104(10), 4303–4418.
- Xu, W., & Wang, Y. (2019). Recent progress on zinc-ion rechargeable batteries. *Nano-Micro Letters*, 11(1), 1–30.
- Yadav, G. G., Turney, D., Huang, J., Wei, X., & Banerjee, S. (2019). Breaking the 2 v Barrier in Aqueous Zinc Chemistry: Creating 2.45 and 2.8 v MnO<sub>2</sub>-Zn Aqueous Batteries. *ACS Energy Letters*, 4(9), 2144–2146.

- Yang, H., Yin, L., Liang, J., Sun, Z., Wang, Y., Li, H., He, K., Ma, L., Peng, Z., Qiu, S., Sun, C., Cheng, H. M., & Li, F. (2018). An aluminum–sulfur battery with a fast kinetic response. *Angewandte Chemie - International Edition*, 57(7), 1898–1902.
- Yoshino, A. (2012). The birth of the lithium-ion battery. *Angewandte Chemie - International Edition*, 51(24), 5798–5800.
- Yuste, A. P. (2008). Salvá's electric telegraph based on Volta's battery. *IEEE History of Telecommunications Conference, HISTELCON 2008, April*, 6–11.
- Zein El Abedin, S., Moustafa, E. M., Hempelmann, R., Natter, H., & Endres, F. (2006). Electrodeposition of nano- and macrocrystalline aluminium in three different air and water stable ionic liquids. *ChemPhysChem*, 7(7), 1535–1543.
- Zhang, N., Cheng, F., Liu, J., Wang, L., Long, X., Liu, X., Li, F., & Chen, J. (2017). Rechargeable aqueous zinc-manganese dioxide batteries with high energy and power densities. *Nature Communications*, 8(1), 1–9.
- Zhang, W., Liang, S., Fang, G., Yang, Y., & Zhou, J. (2019). Ultra-high mass-loading cathode for aqueous Zinc-ion battery based on graphene-wrapped aluminum vanadate nanobelts. *Nano-Micro Letters*, 11(1), 1–12.
- Zhao, Q., Zachman, M. J., Al Sadat, W. I., Zheng, J., Kourkoutis, L. F., & Archer, L. (2018). Solid electrolyte interphases for high-energy aqueous aluminum electrochemical cells. *Science Advances*, 4(11), 1–8.
- Zhongfei, W., Yu, L., Chengzhi, D., Haimin, Z., Ruirui, Z., & Hongyu, C. (2020). The critical role of boric acid as electrolyte additive on the electrochemical performance of lead-acid battery. *Journal of Energy Storage*, 27, 1–7. doi:10.1016/j.est.2019.101076.
- Zhu, J., Hihara, L. H. (2010) Corrosion of continuous alumina-fibre reinforced Al–2 wt.% Cu–T6 metal–matrix composite in 3.15 wt.% NaCl solution, *Corrosion Science*, 52, 406–415.